DEUTSCHES ELEKTRONEN-SYNCHROTRON DESY

DESY 83-088
September 1983

HIGH p_T REACTIONS IN PHOTON-PHOTON COLLISIONS

by

A. Deuter
Deutsches Elektronen-Synchrotron DESY, Hamburg
and
I. Physikalisches Institut, RWTH Aachen

PHOTON STRUCTURE FUNCTIONS AND DETERMINATION OF α_s

by

W. Wagner
I. Physikalisches Institut, RWTH Aachen

RESONANCES IN TWO-PHOTON SCATTERING

by

E. Hilger
II. Institut für Experimentalphysik, Universität Hamburg

Q^2 DEPENDENCE OF SINGLE MESON PRODUCTION IN $\gamma\gamma$ COLLISIONS

by

M. Poppe
II. Institut für Experimentalphysik, Universität Hamburg

ISSN 0418-9833

NOTKESTRASSE 85 · 2 HAMBURG 52

To be sure that your preprints are promptly included in the
HIGH ENERGY PHYSICS INDEX ,
send them to the following address (if possible by air mail) :

DESY
Bibliothek
Notkestrasse 85
2 Hamburg 52
Germany

DESY 83-088
September 1983

ISSN 0418-9833

HIGH p_T REACTIONS IN PHOTON-PHOTON COLLISIONS

Armin Deuter
DESY, Hamburg and I. Physikal. Institut, RWTH Aachen

PHOTON STRUCTURE FUNCTIONS AND DETERMINATION OF α_s

Walter Wagner
I. Physikalisches Institut, RWTH Aachen

RESONANCES IN TWO-PHOTON SCATTERING

Erwin Hilger
II. Inst. f. Experimentalphysik, Universität Hamburg

Q^2 DEPENDENCE OF SINGLE MESON PRODUCTION IN $\gamma\gamma$ COLLISIONS

Martin Poppe
II. Inst. f. Experimentalphysik, Universität Hamburg

Contributions to the Two-Photon Session at the
XIV International Symposium on Multiparticle Dynamics,
Granlibakken, Lake Tahoe, USA, June 22 - 27, 1983

High P_t Reactions in Photon Photon Collisions

Armin Deuter *

Deutsches-Elektronen-Synchrotron DESY, Hamburg

Introduction

The basic diagram for hadron production by the two photon mechanism is shown in Figure 1.

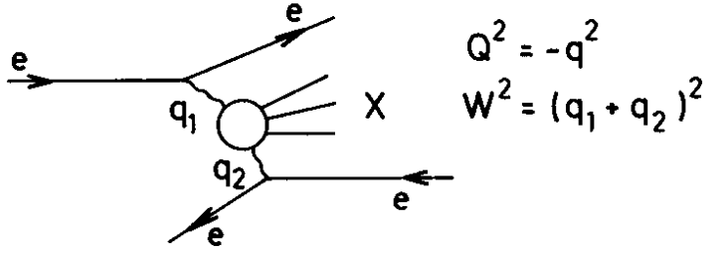

Figure 1. Feynman diagram for $e^+e^- \to e^+e^- + X$

* Now at I. Physik. Inst. RWTH Aachen

The two incoming electrons radiate photons which react and produce a final state X. The bulk of the reactions is expected to be due to the diffractive $\rho\rho$ scattering (Figure 2)

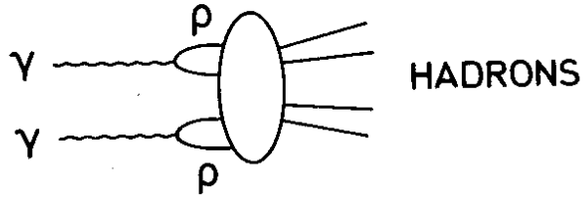

Figure 2. $\gamma\gamma \to \rho\rho \to$ hadrons

producing final state particles dominantly in forward backward directions, with an exponential fall off of the transverse momenta.($\sim e^{-AP_t}$). But in addition to that the photon has a hard component, coming from the direct quark photon coupling. (see Figure 3)

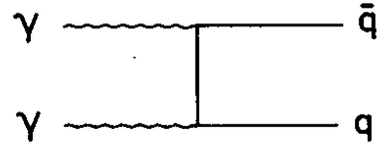

Figure 3. Box diagram for $\gamma\gamma \to q\bar{q}$

If the exchanged quark is highly virtual this leads to a very particular event signature: Two outgoing electrons at small angles and two hadronic jets at large transverse momenta.

This process is calculable with the hard scattering expansion/1/

The remarkable features of this process are:

- Proportionality to the sum of the quark charges to the fourth power
- $1/P_t^4$ dependence (P_t being the transverse momentum of the quarks relative to the beam axis)

This P_t behavior of the underlying hard process on the parton level is reflected in the same power law of the jets and the single particle distributions.

Common Selection Criteria

Experimental investigations have been made by the groups CELLO, JADE, PLUTO and TASSO at the e^+e^- storage ring PETRA. In the following some typical cuts will be described: Momentum balance, charge balance and a cut in the invariant mass W ($W < 1/3\ E_{beam}$) are necessary to get rid of the large background. For a reasonable jet analysis $W > 4$ GeV and at least four tracks are needed.

Background

The most dangerous background besides $\gamma\gamma \to \tau\bar{\tau}$ and beam gas events is the one γ anihilation channel. In the single tag case the two and one γ events are separated due to the different signature of the reactions: The two photon events have in addition to a hadronic final state a high energetic outgoing electron detected at small angles. If it is possible to identify this electron with a tracking

device or a Čerenkov counter the separation will be perfect. But if the electrons are detected using only shower information photons look like electrons. One γ events with one radiated photon from the initial state may simulate a $\gamma\gamma$ reaction and are therefore a severe background at high invariant masses and low tag energies.

The situation becomes more difficult in no tag reactions where only the final state is measured. A cut in the invariant mass separates one γ and two γ events. In two photon physics W is a small fraction of the CMS energy while in the anihilation channel W is equal to $2*E_{beam}$. But due to particle losses and resolution effects W is smeared out and shifted to lower W values.

In Figure 4 the distribution of the momentum sum of charged particles /2/ (which is a measure of W) divided by the beam energy demonstrates to which extend the two processes can be separated.

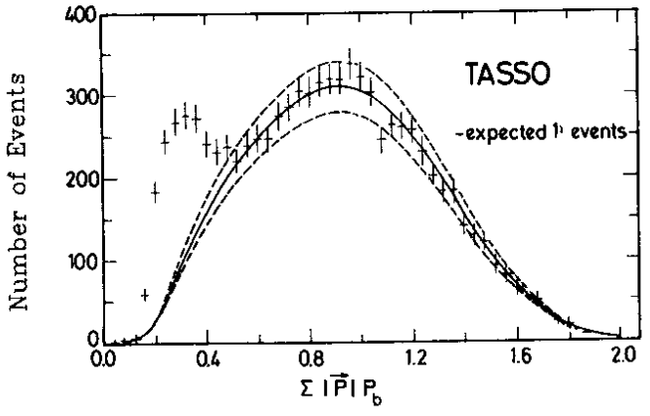

Figure 4. $\sum P$ / beam momentum

For a reliable subtraction a good MC-simulation (full line) is essential.

Experimental Results

In Figure 5 the inclusive P_t^2 distributions of hadrons relative to the beam axis are shown for the single tag analysis of TASSO /3/ and PLUTO.

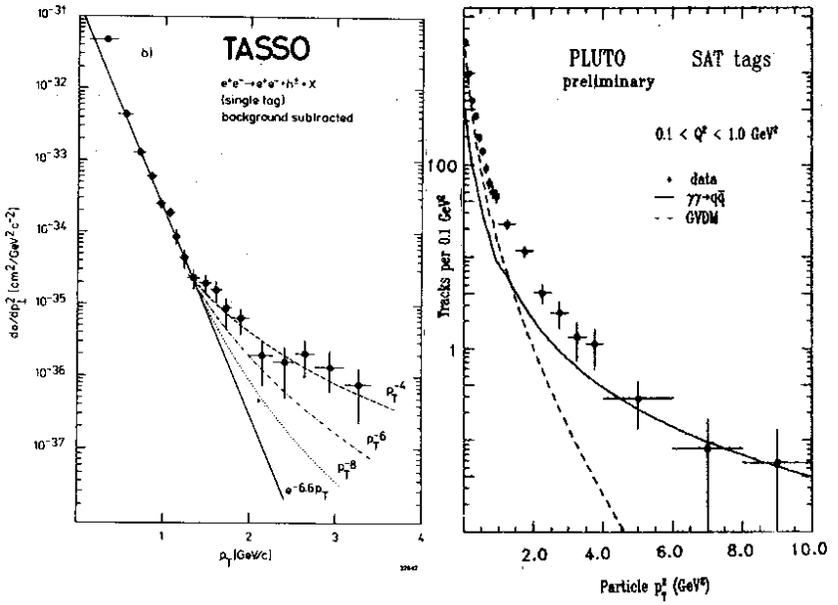

Figure 5. Inclusive Pt distribution of hadrons

The TASSO data show an exponential fall off up to 1 GeV^2 ($\sim e^{-6.6\ Pt}$) and follow a power law ($\sim P_t^{-4}$) at high P_t. This is exactly the behavior one would expect from the superposition of the VDM and the pointlike component of the photon.

In the PLUTO analysis the data have been compared to the absolute prediction of these two models using a limited phase space proportional to $e^{-5\ Pt^2}$ for the VDM model/4/. It looks as if two times the quark model + VDM would be a perfect description of the data.

In the TASSO notag analysis /2/ the data are presented after subtraction of the one photon background and the VDM component. In Figure 6 the maximum P_t of the event is compared to the quark model prediction. In the whole P_t range a factor of 4 would be needed to describe the data.

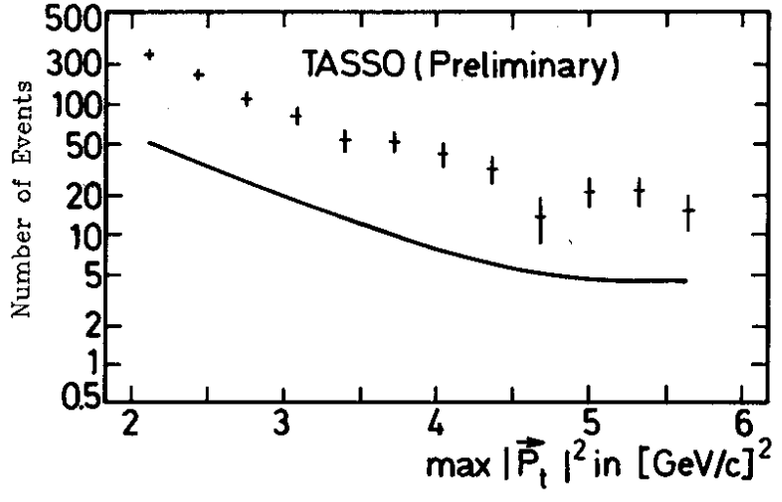

Figure 6. Pt^2 distribution of particle with max. Pt

Jet Analysis

Jet searching in $\gamma\gamma$-physics has special problems. The jets are broad because of the low invariant mass and the LAB frame does not coincide with the CMS frame. They are therefore not collinear. For the

reconstruction of jets PLUTO and TASSO used a twoplicity method, CELLO and JADE a cluster algorithm which allows for more than two jets. The scatter plots /5/ (Figure 7) demonstrate a strong correlation between the quark axis and the jet axis.

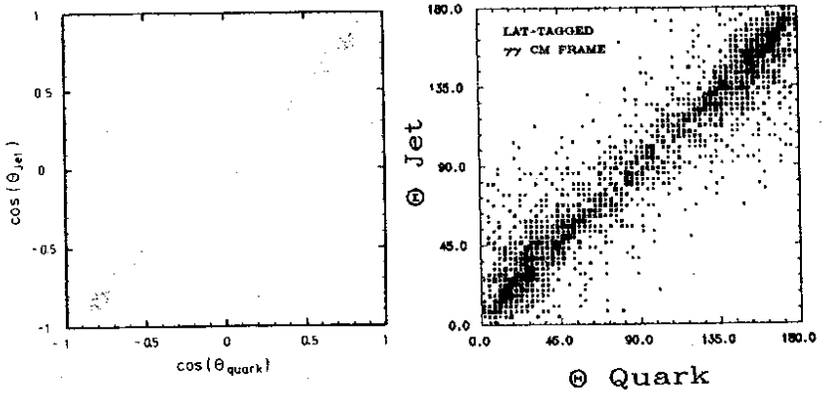

Figure 7. Correlation between quark and reconstructed jet axis

In Figure 8 the P_t distributions of jets measured by JADE /6/ and TASSO /3/ are shown. A similar behavior as described in the single particle distributions is observed: The data are not described by the VDM part alone (see full and dotted line) and follow the prediction of the quark model for $P_t > 3$ GeV. But even at the highest available P_t values of about 6 GeV the data are systematicly higher than the basic QM process.

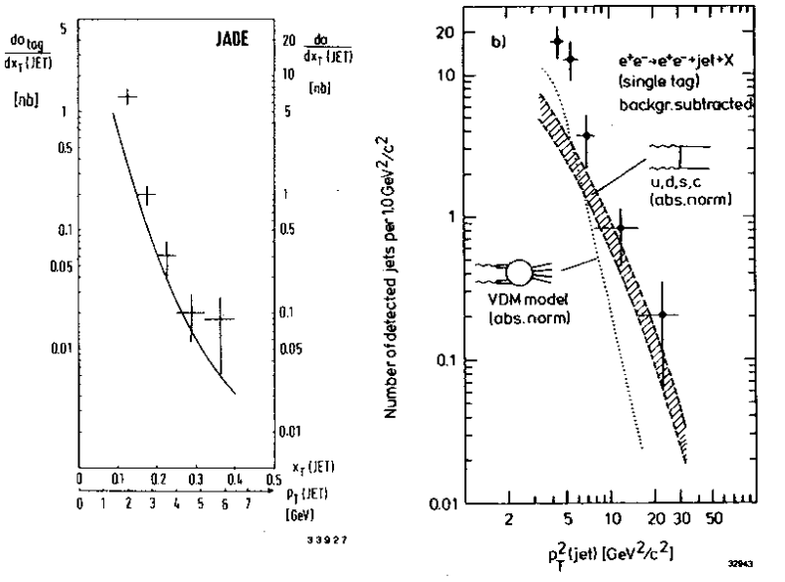

Figure 8. Pt distribution of jets

This excess can be expressed more quantitative by introducing the ratio $\tilde{R}_{\gamma\gamma}$ between observed hadronic events and predicted $\gamma\gamma \to q\bar{q}$ events. $\tilde{R}_{\gamma\gamma}$ versus P_t is plotted in Figure 9 for 5 Q^2 bins.

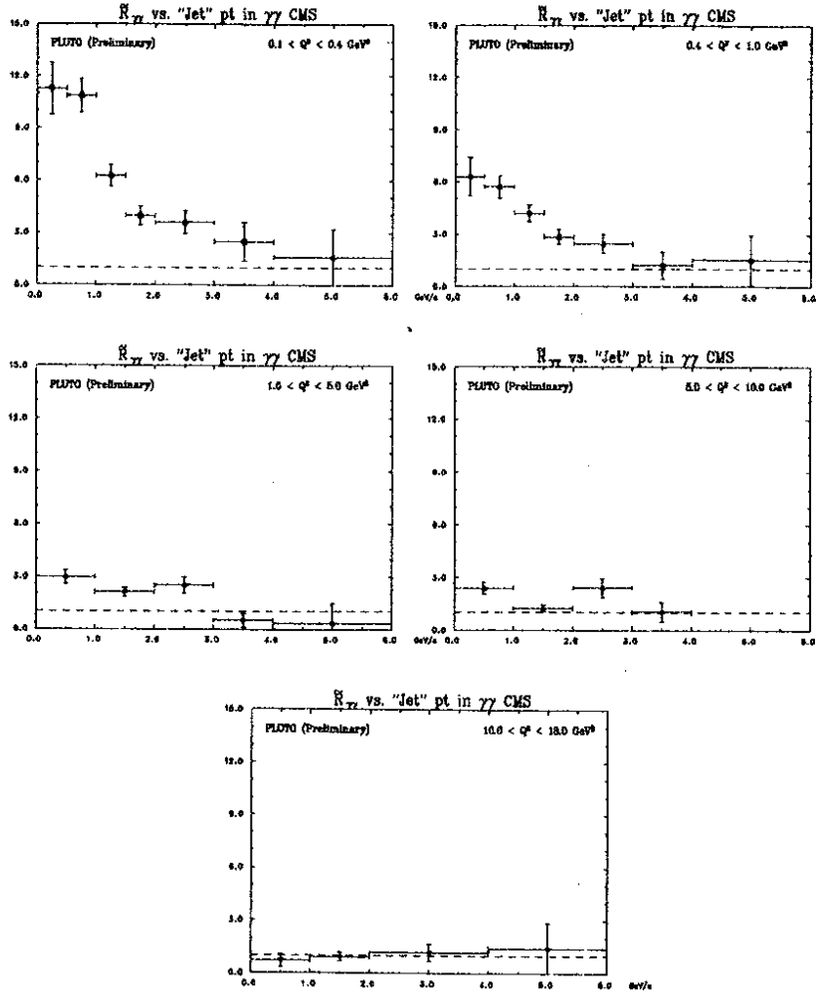

Figure 9. $\tilde{R}_{\gamma\gamma}$= observed events / predicted $\gamma\gamma \rightarrow q\bar{q}$ events

At low P_t and low Q^2 the data are substantially higher than the quark parton prediction. Wether the VDM part alone or in addition multi jet events or QCD effects contribute to the excess is still under investigation. But the excess in the data approaches 0 with increasing P_t or increasing Q^2. It appears that the QPM describes the process totally if only one momentum transfer gets hard.

An analysis of the final state may help to separate the different basic processes. A first step in that direction is a thrust analysis in two Q^2 bins.(Figure 10)

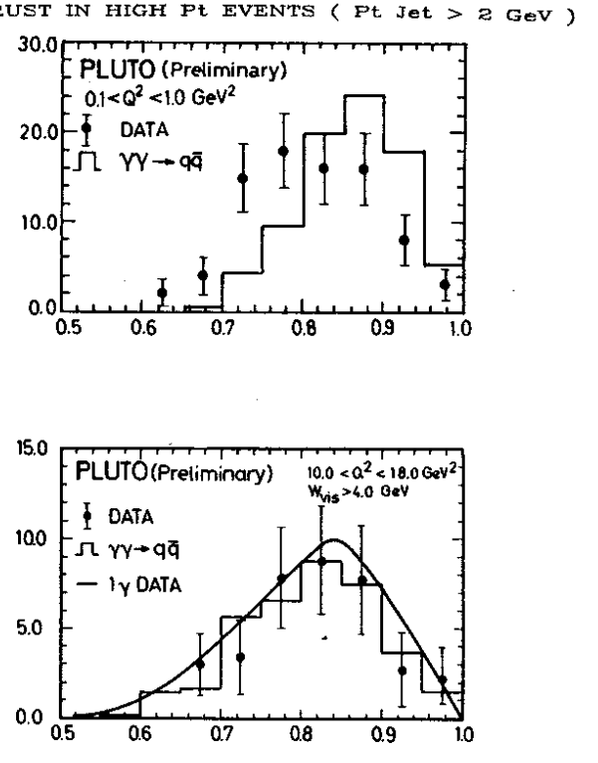

Figure 10. Thrust of jet events in two Q^2 bins

In the lower Q^2 bin the events look more isotropic than the $\gamma\gamma \to q\bar{q}$ MC predicts. With increasing Q^2 the events become more jetlike in agreement with the QPM prediction.

PLUTO has the nice opportunity to compare the thrust distributions of 1 γ anihilation data (full line in Figure 10) taken at DORIS with 2 γ events at a similar invariant mass range (W~9 GeV). The good agreement demonstrates that in one and two photon physics the jets look similar.

From these distributions it is obvious that the excess at low Q^2 is not dominated by a two jet final state but more isotropic topologies like multi jet events or not fully reconstructed difractiv events are needed.

Conclusions

In two photon physics pointlike reactions occur at lower transverse momenta (P_t>2) than in hadron hadron collisions /7/.

The quark parton model describes the data at high P_t or high Q^2 in the absolute cross section as well as in the event topology. In the low Q^2 low P_t region an excess of data with an isotropic event signature is observed.

The measurement of $\tilde{R}_{\gamma\gamma}$ rules out the naive integral charged quark model ($\tilde{R}_{\gamma\gamma}^{ICQ} = 2.6$). But in a dynamical ICQ theory /8/ $\tilde{R}_{\gamma\gamma}^{ICQ}$ is expected to be unity in the measured Q^2 range. For a sensitive test a measurement of $\tilde{R}_{\gamma\gamma}$ at low Q^2 (no tag) for clear two jet events is needed.

Acknowledgment

I would like to express my thanks to all my PETRA colleagues, and in particular to Susan Cartwright and Allan Tylka, for many useful discussions of their data. I would also like to thank G. Gunion and R. Lander for the stimulating and enjoyable atmosphere of this conference.

References

/1/ S.M. Berman, J.D. Bjorken and J.B. Kogut, Phys. Rev. D4(1971) 3388
/2/ E. Duchovni, talk given at the 5. Int. Workshop on Photon Photon Collisions, Aachen(1983)
/3/ TASSO Collaboration, R. Brandelik et al.,Phys.Lett. 107B (1981) 290
/4/ I.F. Ginzburg and V.G. Serbo Phys.Lett. 109B (1982) 231
/5/ N. Wermes, Thesis Bonn 1982, BONN-IR-82-27
/6/ JADE Collaboration, W. Bartel et al.,Phys.Lett. 107B (1981) 163
/7/ UA1 Collaboration Cern EP/82-174
/8/ M.Y.Han and Nambu, Phys. Rev. 139(1965) B1006
J.C. Pati and A.Salam, Phys. Rev. D8(1973) 1240
J.C. Pati and A.Salam, Phys. Rev. D10(1974) 275

PHOTON STRUCTURE FUNCTIONS AND DETERMINATION OF α_s

Walter Wagner

1. Phys. Inst. RWTH Aachen
Sommerfeldstr., D51 Aachen
Germany

ABSTRACT

The experimental results on the photon structure function F_2 in the Q^2 range from 1 - 300 GeV^2 are reviewed. The preliminary data are in nice agreement with QCD predictions, using $\Lambda \approx 200$ MeV. The first steps to measure the structure functions F_1 and F_3 are described.

1. Introduction

Hadron production by the two photon mechanism in e^+e^- storage rings (Fig. 1) is certainly a complicated thing. The total differential cross

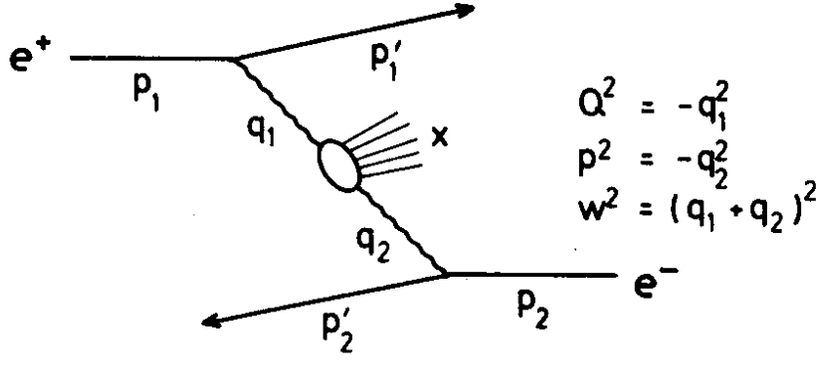

Fig. 1 Kinematics of the two photon reaction

section for unpolarized electron beams is given by the expression[1)]

$$\frac{d\sigma}{d\Gamma} = L^{TT}\,\sigma_{TT} + (L^{TL}\,\sigma_{TL} + L^{LT}\,\sigma_{LT}) + L^{LL}\,\sigma_{LL} + \tilde{L}^{TT}\,\tau_{TT}\cdot\cos 2\phi + \tilde{L}^{TL}\,\tau_{TL}\cos\phi \,. \qquad (1)$$

The luminosity functions L, $\tilde{L}$ for the transverse and longitudinal photon fluxes are well known and calculable in QED. The σ's are the cross sections of interest and the τ's are interference terms with ϕ being the angle between the electron and the positron scattering planes. Using the obvious relation $\sigma_{TL}(W^2, q_1^2, q_2^2) = \sigma_{LT}(W^2, q_2^2, q_1^2)$ we are left with five measurable quantities as a function of three variables W^2, q_1^2, q_2^2.

This is quite an extensive experimental program and after almost five years analysis at DESY and SLAC we are just at the beginning. Almost all results have been obtained in the single tag mode (where only one of the outgoing electrons has been detected). In this set up the measurable quantity is the sum of $\sigma_{TT} + \varepsilon\,\sigma_{TL}$ which can be studied as a function of W and Q^2 (= $-q_1^2$, say). If Q^2 is large enough, say $Q^2 \gg m_\rho^2$, it is more appropriate to interprete the data in terms of photon structure functions rather than photon-photon cross sections. The asymmetric configuration very much looks like deep inelastic electron scattering off an almost real photon target (Fig. 2).

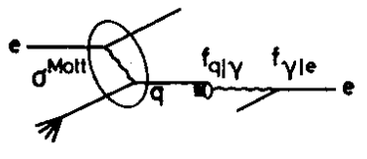

$$\frac{d\sigma^{Mott}}{dQ^2} = \frac{4\pi\alpha^2}{Q^2}\,\frac{s^2+u^2}{2s^2} = \frac{4\pi\alpha^2}{Q^4}\,(1-y+\frac{y^2}{2})$$

Fig. 2 Deep inelastic electron photon scattering

In the quark picture the process is simply given by the elastic electron quark scattering multiplied by the probability to find a quark inside a photon $f_{q/\gamma}(x)$ times the probability to find a photon inside an electron $f_{\gamma/e}(z)$:

$$\frac{d^2\sigma}{dQ^2 dx} = \frac{4\pi\alpha^2}{Q^2}\left(1-y+\frac{y^2}{2}\right)\underbrace{\sum_{q+\bar{q}} e_q^2 \cdot f_{q/\gamma}(x)}_{\frac{1}{x}F_2^\gamma(x)} \cdot f_{\gamma/e}(z)dz \qquad (2)$$

Thus the photon structure function F_2 has the very intuitive meaning of (x times) the momentum distribution of quarks inside a photon. If longitudinal terms are kept, eq. (4) reads more precisely

$$\frac{d^2\sigma}{dQ^2 dx} = \frac{4\pi\alpha^2}{Q^4}\,\frac{1}{x}\,\{(1-y)\,F_2 + xy^2\,F_1\}\,f_{\gamma/e}(z)dz \qquad (3)$$

The formal connection of cross sections and structure functions is given by

$$2\,x\,F_1 = \frac{Q^2}{4\pi^2\alpha}\,\sigma_{TT}$$
$$F_2 = \frac{Q^2}{4\pi^2\alpha}\,(\sigma_{TT} + \sigma_{TL}) \qquad (4)$$

and the scaling variables x, y, z are defined by

$$x = \frac{-q_1^2}{2q_1q_2} = \frac{Q^2}{Q^2+W^2} \approx \frac{E_q}{E_\gamma}$$
$$y = \frac{q_1q_2}{q_1q_2} = 1 - \frac{E'}{E}\cos^2\frac{\theta}{2} \approx \frac{E_\gamma^1}{E} \qquad (5)$$
$$z = \frac{E_\gamma^2}{E}$$

with the meaning of fractional momenta of one particle inside another.

2. Structure Function $F_2(x, Q^2)$ of a Real Photon

The investigation of deep inelastic eγ scattering made a big step forward in the last two years. In 1980 we had roughly 100 hadronic events[2] in the Q^2 range from 1 - 15 GeV². The first indication that these rather small values are already large enough came from the Q^2 dependence of the total cross section, which was in definite disagreement

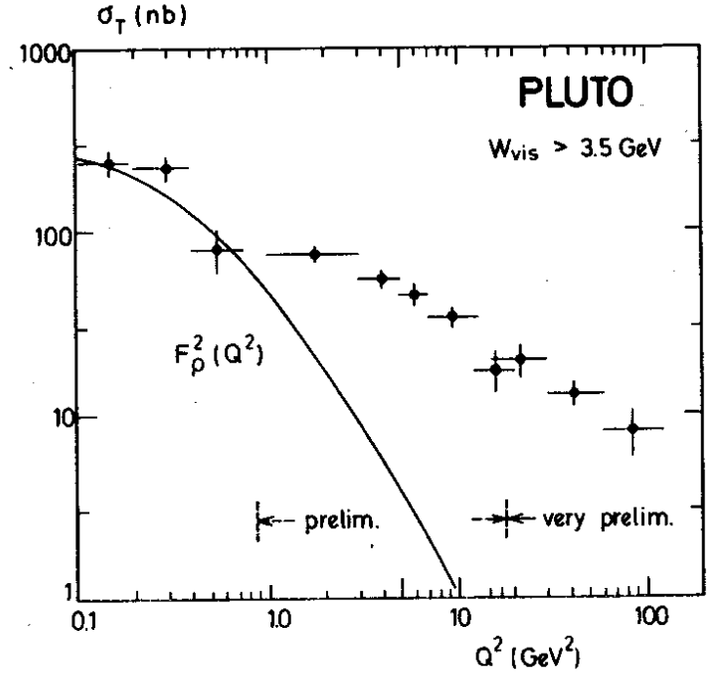

Fig. 3 Q^2 dependence of the total γγ cross section. The solid curve represents the ρ pole formfactor

with a simple ρ-pole formfactor above 2 GeV (fig. 3 includes the new data with high statistics). The VDM, however, turned out to be flexible enough to describe the Q^2 dependence in a natural way by including higher vector mesons (GVDM)[3]. But the interpretation of this weak Q^2 fall off as the onset of the deep inelastic regime got support from the final state analysis. Fig. 4 shows the p_T^2 distribution of reconstructed jets for single tag events in different Q^2 regions[4] (the index T refers to the transverse direction in the γγ CMS). At small Q^2 ($Q^2 < 1$ GeV²) the QM accounts only for a small fraction of the events and describes only the high p_T tail quantitatively. At large Q^2 a large fraction of the data follows the QM prediction. The natural explanation of this behaviour is that we start seeing the direct photon quark coupling so that the process is better understood as deep inelastic electron photon scattering. The quantity to measure in this case is the photon structure function $F_2^\gamma(x, Q^2)$

$$F_2^\gamma(x, Q^2) = 2\,x\,\sum_q e_q^2\,f_{q/\gamma}(x, Q^2). \qquad (6)$$

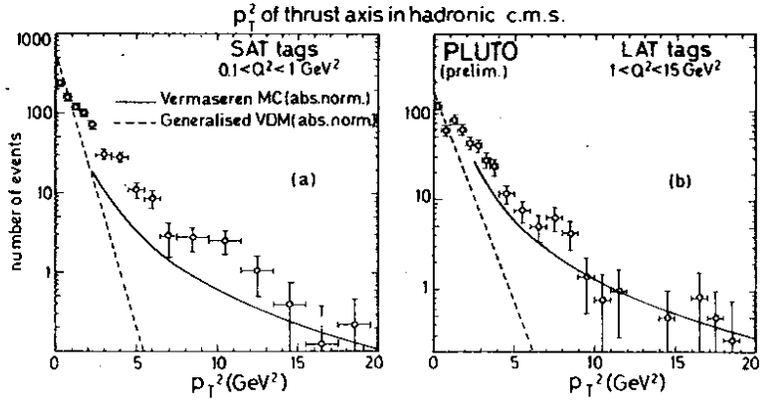

Fig. 4 p_T^2 distribution of the reconstructed jets compared to VDM and QM predictions for small a) and large b) Q^2

Predictions. What are the models for F_2^γ, or in other words, what is the quark content of a photon? In a very simplified picture the process proceeds as follows: At pointlike distances the photon splits into a $q\bar{q}$ pair and the two quarks fly apart. This vertex is straight

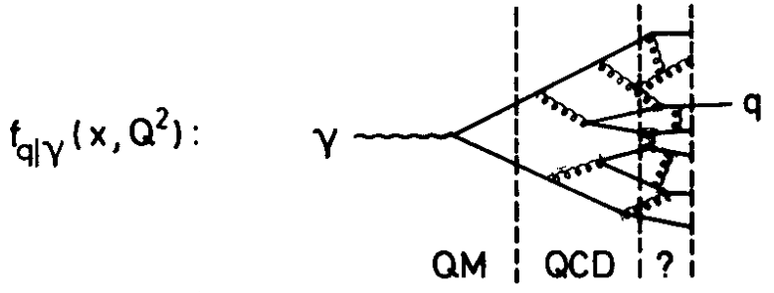

Fig. 5 Quark gluon cascade

forward calculable in the QM. At larger distances the gluon effects get more and more important up to the point where perturbative QCD breaks down. In momentum space this picture corresponds to a p_T integration

over the available phase space:

$$\int_0^{Q^2} \frac{dp_T^2}{p_T^2 + 0(m^2)} = \int_0^{\Lambda^2} \frac{dp_T^2}{p_T^2 + 0(m^2)} + \int_{\Lambda^2}^{Q^2} \frac{dp_T^2}{p_T^2 + 0(m^2)} \quad (7)$$

I II

The first part of this integral is not calculable in perturbative QCD. This is bad but there may be three ways out. First we can hope that a full QCD, including lattice calculations, can solve this integral. Second we can go to extremely large Q^2 values so that the relative importance of part I vanishes. Third we can call this integral the hadronic piece of the photon and try to extract that piece from hadronic structure functions. The motivation for that is that a typical value of Λ is not very much different from the inverse hadronic radius. The second part can be calculated in a straight forward way if Q^2 is large enough[5]. The result is a structure function that rises proportional to $\ln Q^2$:

$$F_2 \sim \ln \frac{Q^2}{\Lambda^2} \sim \frac{1}{\alpha_s} \quad \text{if } \Lambda^2 \gg m^2$$
$$(8)$$
$$F_2 \sim \ln \frac{Q^2}{0(m^2)} \quad \text{if } \Lambda^2 \ll m^2 .$$

The photon structure function is unique in many respects:

1. it is expected to rise with x unlike all other hadronic structure functions
2. it should have a strong positive scale breaking effect $\sim \ln Q^2$
3. the absolute normalization of the dominant part is predicted by QCD
4. the absolute normalization is very sensitive to α_s and Λ ($1/\alpha_s$ as compared to $(1 + \alpha_s/4\pi)$ in e^+e^- annihilation).

Especially the last point made many people (experimentalists and theoreticians) enthusiastic about the photon structure function. A determination of Λ to a 30% accuracy seemed to be possible from an experimental point of view (see discussion below). However, this optimistic situation has changed recently. In addition to the problems at small x and in the region $x \approx 1$ there are now singularities entering the game as severe as $x^{-5.33}$ poles. These singularities wait for cancellations which are not calculable in the moment. Thus the whole beauty of the photon structure function would be destroyed. But it is not clear whether one has to be all that pessimistic[7]. We have got

used to all sorts of singularities which we don't have to worry about. And we know from recent calculations by Uematzu and Walsh[8] that for the case of the virtual photon the singularities don't play a role if $-q_1^2 = p^2 \gg \Lambda^2$. In this case the denominator in eq. 7 gets an additional mass scale, p^2, and the integral gets the form

$$\ln \frac{Q^2}{p^2} . \qquad (9)$$

This is a safe QCD prediction but the parameter Λ hides behind the larger mass scale in the same way as it does for heavy quarks. So let us hope that there will be a smooth transition from the case of the virtual structure function to the real structure function and that there finally will be a meaningful QCD prediction to be compared with experimental measurements. Fig. 6 summarizes the expectations for $F_2(x)$ (for a detailed discussion of the hadronic part see e.g. ref.[9]). For small Q^2, say $Q^2 < 5$ GeV^2, the pointlike and the hadronic part add up to a more or less constant structure function, whereas for large Q^2, say $Q^2 > 20$ GeV^2, $F_2(x)$ rises with x.

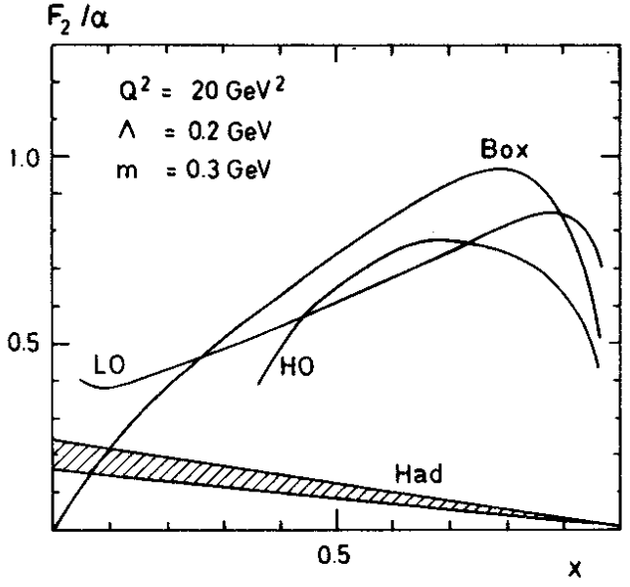

Fig. 6 Predictions for the photon structure function: Hadronic part (Had), QCD calculations in leading order (LO) and higher order (HO) and the quark model (Box)

First results. The first results on F_2 (x, Q^2), obtained by PLUTO three years ago[2], show good agreement of the data with a simple superposition of QCD and the hadronic part, if Λ is of the order of 200 MeV (see fig. 7). Though this measurement is based on roughly 100 events only, it has shown that the photon has somewhat more than a hadronic component only. A first result from JADE[17] showed that the structure function at higher Q^2 of 23 GeV^2 is dominated by the QCD contribution.

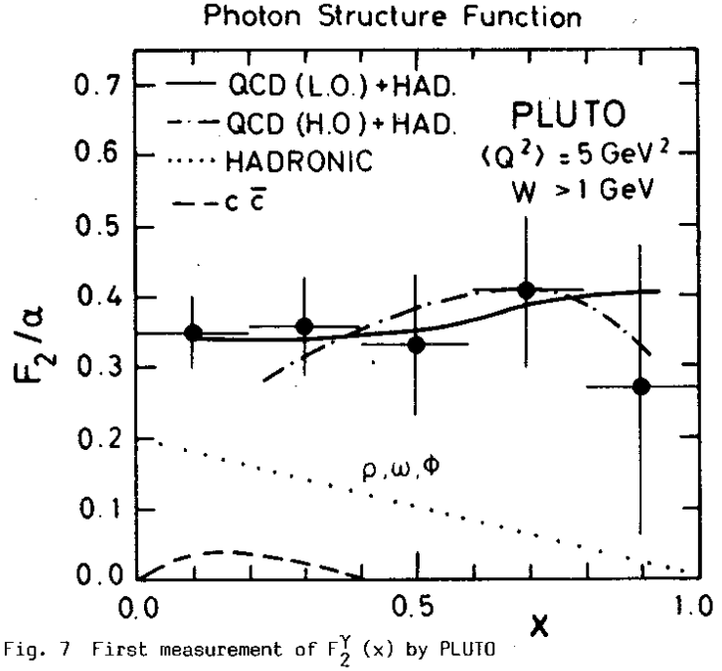

Fig. 7 First measurement of F_2^γ (x) by PLUTO

Before I discuss the new experimental data I want to summarize the experimental data I want to summarize the experimental problems which we have to deal with.

Statistics. The experiments made a big step forward as far as statistics is concerned. The situation is summarized in Tab. 1. The 2000 events from PLUTO, e.g. would allow a measurement of F_2 (x, Q^2) in 4 Q^2 and 5 x bins, with a statistical error of about 10% in each bin. It is also interesting to note that the Q^2 range has extended up to 300 GeV^2!

Table 1

experiment	events	Q^2 range	$\langle Q^2 \rangle$ [GeV^2]
CELLO	200	3 - 300	9
JADE	400	10 - 55	24
JADE	45	40 - 220	100
MAC	150		32
PLUTO	2000	1 - 18	6
PLUTO	120	15 - 150	45
TASSO	200	10 - 50	23

Fragmentation. Only for an ideal detector with 4π coverage the process does not depend on the fragmentation model used. For any realistic detector, however, the detection efficiency depends on fragmentation and therefore the corrections are model dependent. Thus the event simulation for a bad detector could look indistinguishable using one model F (x, Q^2) with a certain fragmentation and a completely different model F (x, Q^2) with a different fragmentation. A detailed Monte Carlo study for the PLUTO detector showed that the situation is not that bad. Due to a good coverage in forward directions the detection efficiency is quite satisfactory (larger than 50% on average, see fig. 8). It turned out that a variation of fragmentation parameters has small effects on the efficiency but can be seen as a large effect in the fragmentation variables. This is

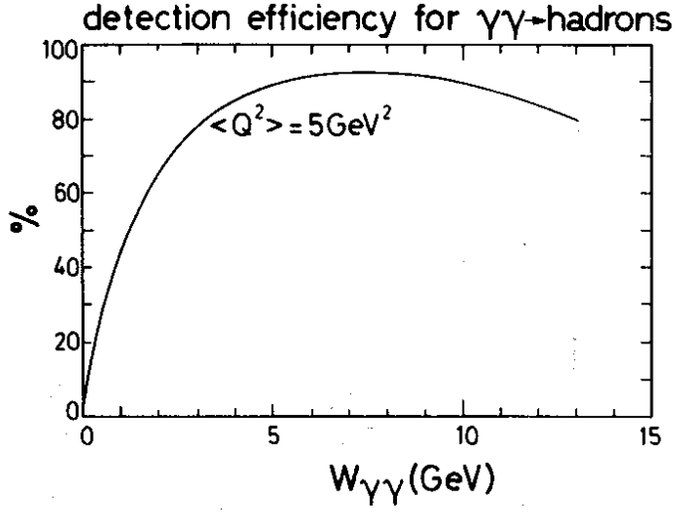

Fig. 8 Detection efficiency of the PLUTO detector

demonstrated in fig. 9 where the effect of the most sensitive variable, the transverse momenta of the particles, is studied. Two very extreme models have been compared, an isotropic phase space model (solid line)

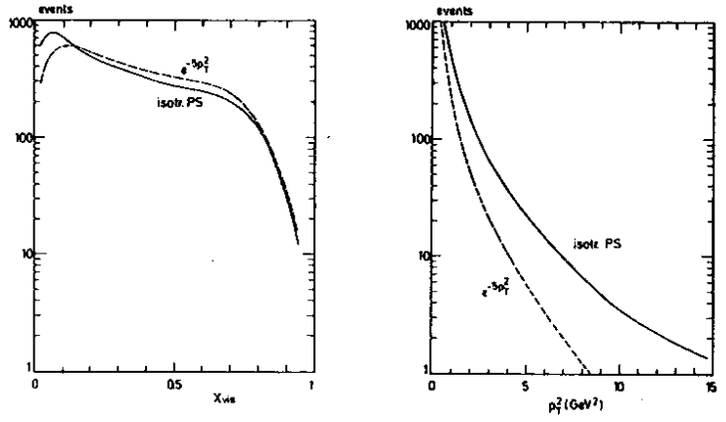

Fig. 9 Effect of the fragmentation variation on a) acceptance (x_{vis}), b) visible p_T^2 distribution

and a limited p_T phase space model, where the particles are collimated jet-like $\exp(-5p_T^2)$ along the $\gamma\gamma$ axes (dashed line). The p_T^2 distributions differ by more than a factor of 2, whereas the effect on the x - distribution (due to differences in the efficiency) is only less than 20%, except for very small x. Thus the remaining uncertainty after adjusting the p_T distribution to the data is estimated to be less than 10%.

Unfolding. In addition to inefficiencies we have the problem of particle losses. Though the event may not be lost completely, the invariant mass of the visible final state, W_{vis}, is smaller than the true W, if one or more particles are not detected. Fig. 10 shows the distribution of the ratio W_{vis}/W as seen in the PLUTO detector. The shaded area represents the situation of PLUTO 1979 without a forward spectrometer. The inclusion of particle detection in the forward region obviously is of great help. The shift in W automatically leads to a shift in $x \rightarrow x_{vis} > x$ which is corrected for in an unfolding procedure. This procedure was presented by V. Blobel at the $\gamma\gamma$ conference in Aachen and is described in ref. [10]. A preliminary estimate of the systematic error, introduced by unfolding, is about 10% or less.

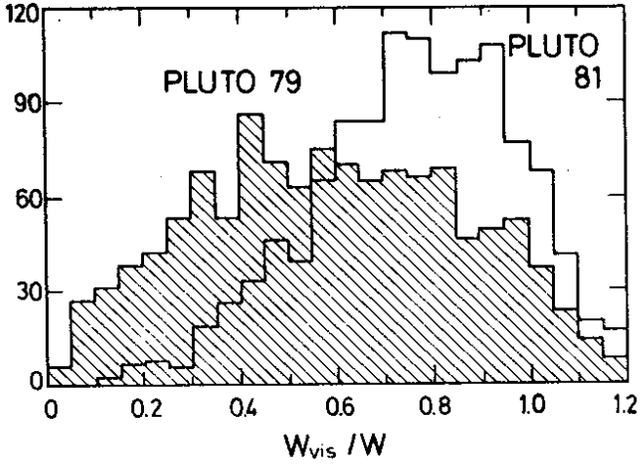

Fig. 10 Ratio of the visible invariant mass and generated invariant mass. The shaded area represents the detector without forward spectrometer

Target mass effects. If the target photon is not restricted to the mass shell by using a good antitagging, the correct treatment of the target mass - $q_2^2 \equiv p^2$ is essential. For $p^2 >> \Lambda^2$ the process has been calculated in ref. 8). The main effect is a change in the log term to $\ln (Q^2/p^2)$. A smooth interpolation to moderate p^2 would thus lead to

$$\ln \frac{Q^2}{\Lambda^2 + p^2} \quad . \tag{10}$$

However it could be that eq. 10 overestimates the effect, as a straightforward QED-calculation results in

$$\ln \frac{Q^2}{\underbrace{m^2 \frac{1-x}{x}}_{\Lambda^2} + x^2 p^2} \rightarrow \ln \frac{Q^2}{\Lambda^2 + x^2 p^2} \quad . \tag{11}$$

If one neglects p^2 in eq. 10 the effect is only minor for an antitag $\Theta < 30$ mrad (5% in α_s and 10% in Λ). But for a loose antitag ($\Theta<100$ mrad) it results in a 15% change in α_s, or 50% change in Λ. Thus one either needs a good antitag or a reliable calculation for the target mass effects in the transition region $p^2 \approx \Lambda^2$.

Heavy quark. For small Q^2 the c-quark contribution is negligible and restricted to small x. As Q^2 increases, however, it gets more and more important and accounts for roughly half the cross section in the limit $Q^2 \rightarrow \infty$. Though this part is not a good tool to determine α_s or Λ, it should be known to an accuracy of about 10% or better. As long as we don't have a QCD calculation for the heavy quarks the best thing to do is to take the QED calculation and subtract it from the data (or add it to the QCD predictions). An alternative way has been tried by PLUTO, where the W-range was restricted to $1.5 < W < 3.5$ GeV[11].

Hadronic component. Even if we are very optimistic about the treatment of the hadronic component of the photon as an additive part to the structure function, we have to worry about uncertainties. The best guess one can try for F_2^{Had}, based on experimental measurements, is given by

$$F_2^{Had}(x,Q^2) = \alpha \cdot (0.2 \pm 0.05)\ (1-x) \tag{12}$$

where scale breaking effects are neglected. This Q^2 independent term can be compensated by another Q^2 independent term coming from QCD by changing Λ to $\Lambda \pm \Delta\Lambda$ in the expression $F_2^{QCD} = h(x) \cdot \ln(Q^2/\Lambda^2)$

$$\Delta F_2^{QCD} = h(x) \cdot \ln \left(\frac{\Lambda \pm \Delta\Lambda}{\Lambda}\right) = \Delta F_2^{Had} \tag{13}$$

$$\frac{\Delta\Lambda}{\Lambda} = \frac{\alpha \cdot 0.05\ (1-x)}{2 \cdot h(x)} \neq f(Q^2) \ .$$

Thus the ignorance about the hadronic component generates an uncertainty in Λ which is independent on Q^2 and which is 40% at $x = 0.4$ and 10% at $x = 0.8$. To conclude, a determination of Λ to ± 30% accuracy seems to be feasible from the experimental point of view. Whether or not this value of Λ is meaningful in the view of the theoretical problems with the singularities has to be answered by theorists.

New results. There are of the order of 3000 hadronic events collected in 5 different experiments, and at least 10 different analyses have been reported at Aachen[10]. I am not going into any details of the trigger conditions, data selection and analysis criteria, but refer to the summary of the parallel sessions instead. However, the analyses have many common features:
Definition of the tag electron by requiring a minimum energy cluster of about E/2 in one of the shower counters.

Definition of the hadronic final state by requiring at least 3 particles. Sometimes the conditions are more restrictive and 3 or 4 charged particles are required, sometimes the class with two charged particles plus neutrals are added.
Antitag is normally applied as far as the detector allows for it.
Q^2 is always determined from the electron and W from the hadronic final state (except for a special analysis of double tag events from PLUTO).

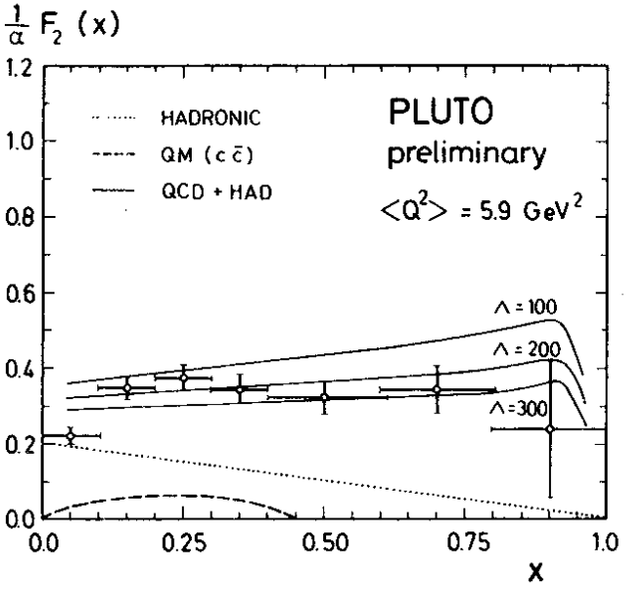

Fig. 11 Unfolded structure function $F_2^\gamma(x)$ at $\langle Q^2 \rangle = 5.9$ GeV^2. The curves are QCD predictions using different values of Λ (PLUTO)

The experiments differ in the way of presenting data. All experiments except PLUTO compare the x_{vis} distribution with model predictions including all detector effects. PLUTO presents the data as an unfolded structure function F(x). The comparison with models can then be done analytically. There is no consistent treatment of the hadronic part, which is neglected in the analysis of JADE, TASSO and MAC, added as $F_2^{Had} = 0.11 \cdot \alpha(1-x)$ by CELLO and added as $F_2^{Had} = 0.2 \cdot \alpha(1-x)$ in the

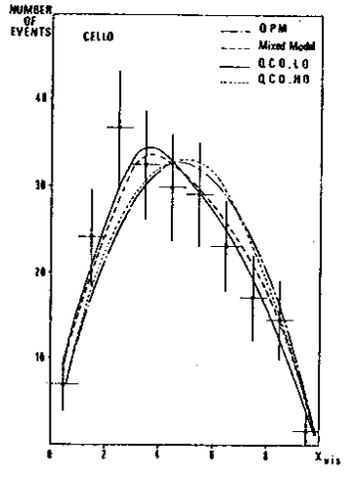

Fig.12 Visible x distribution compared with model predictions (CELLO)

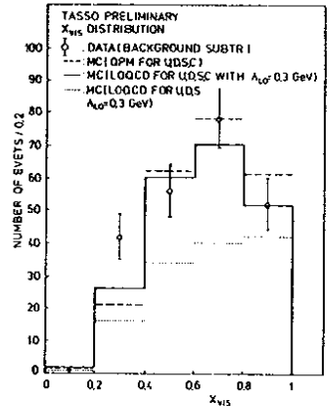

Fig.13 Visible x distribtuion compared with model predictions (TASSO)

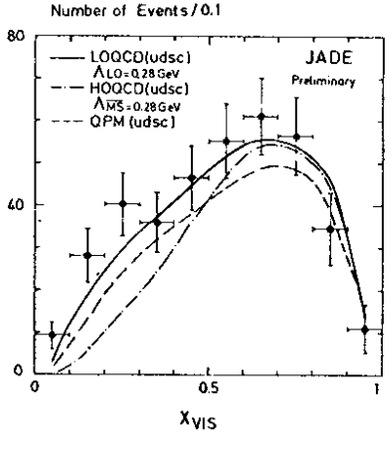

Fig.14 Visible x distribution compared with model predictions (JADE)

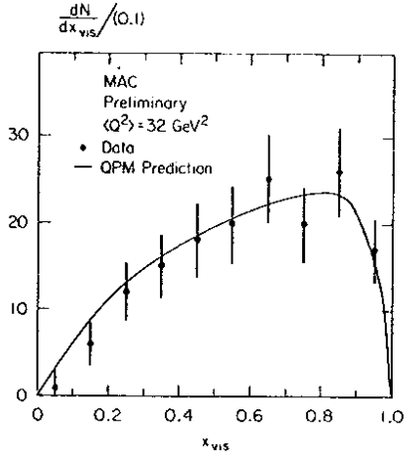

Fig.15 Visible x distribution compared to the (normalized) quark model prediction (MAC)

PLUTO analysis.

In Fig. 11 the PLUTO result is shown. The unfolded structure function $F_2^{\gamma}(x)$ is compared to leading order QCD predictions for different values of Λ. The data are in nice agreement with the superposition of the hadronic part plus the QCD part using $\Lambda \approx 200$ MeV. One also gets a feeling for the sensitivity to a variation of Λ. It is interesting to note that the data are also described by the QM plus hadronic piece but that a rather large quark mass of about 300 to 500 MeV is required (current quark masses of the order of 10 MeV can be ruled out). In Figs. 12 - 16 the x_{vis} distributions are shown for CELLO[12], TASSO, JADE, MAC and PLUTO[13]. In each case the electron has been measured in the endcap shower counter. The data are in good agreement with the QM but also with leading order QCD calculations, which are slightly favoured. The TASSO data demonstrate nicely that at larger Q^2 values the charm contribution is definitely needed.

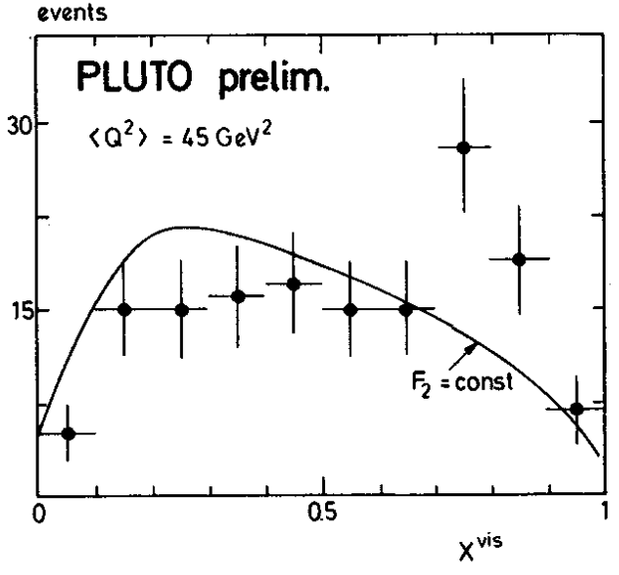

Fig. 16 Visible x distribution compared to the model F_2 = const. (PLUTO)

In the first three figures the data have the tendency to be above the curves at low x, indicating some room for hadronic contributions even at large Q^2. (In the case of CELLO there is room for more than the used contribution $\alpha \cdot 0.11\ (1-x)$). The MAC data are compared with the shape of the QM, where the normalization is adjusted to the data. From the good agreement one can conclude that at these large Q^2 values (32 GeV²) F_2^{γ} definitely rises with x. The same effect can be seen by the comparison of the high Q^2 PLUTO data with a constant structure function (Fig. 16).

The JADE group presented a result at a breathtaking average Q^2 value of 100 GeV², based on roughly 45 events. The electron has been measured at very large angles, around 90°, in the barrel shower counter. The event distribution is plotted in Fig. 17 and perfectly agrees with the leading and higher order QCD calculation, with Λ = 70 MeV. However the errors are that large that a Λ-value of 200 MeV is off by only one standard deviation.

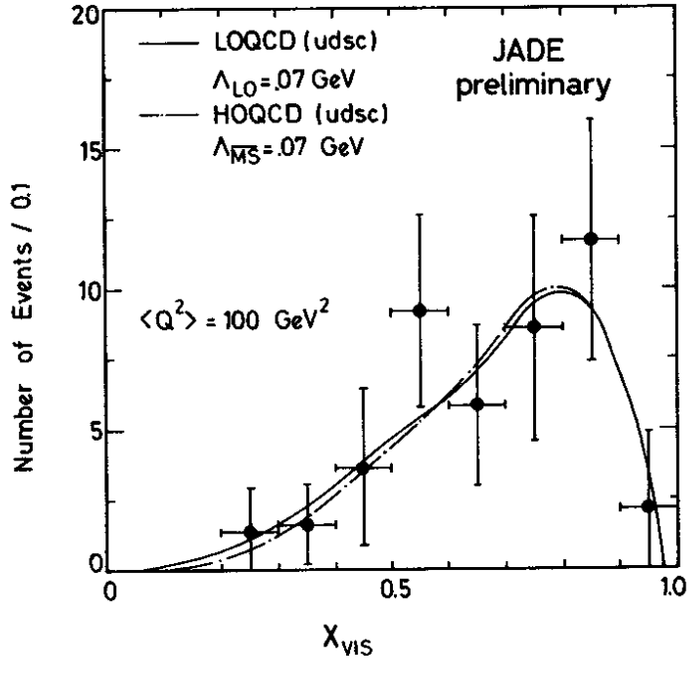

Fig.17 Visible x distribution compared to leading order QCD, Λ = 0.07 GeV (JADE)

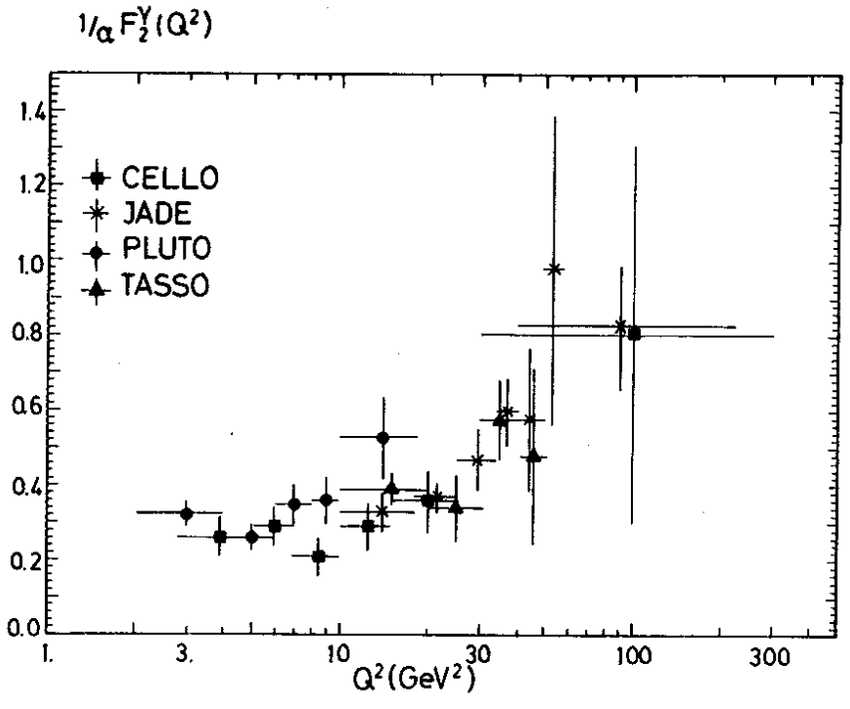

Fig. 18 Q^2 evolution of the photon structure function. The data are averaged over slightly different x ranges for the different experiments

The Q^2 evolution of the photon structure function has been analysed over a phantastic range from $2 < Q^2 < 300$ GeV^2. Each experiment averaged the data over a certain range in x_{vis}, e.g. $0.2 < x_{vis} < 0.8$, or $x_{vis} > 0.3$ or something similar, and plotted the result as a function of Q^2. The compiled data are shown in Fig. 18. There is no doubt that the structure function rises with Q^2, but it is very hard to judge from this figure how much of the effect is due to the logarithmic scale breaking. First of all the experimental cuts in x_{vis} are different in each experiment. But even if the experiments would agree on the same cuts, there are still $x - Q^2$ correlations left which can only be avoided if the data are compared at fixed x (or a small x-bin). These correlations can simulate a rise with Q^2 as the mean value of x in a large x-bin depends on Q^2. In addition to that a large increase of $F_2(Q^2)$ is simply due to the onset

of the charm threshold. Thus one possible scenario would be that each experiment presents $F_2(Q^2)$ at a fixed x, with the charm contribution subtracted. These results could be compared to a universal curve. As this procedure would probably need some more statistics, the experiments use a different technique. They compare the $F_2(Q^2)$ measurements with model calculations where the detector effects, Q^2-x correlations and charm contributions were taken into account. They all find consistency with an increase as predicted by QCD using $\Lambda \approx 200$ MeV. It would be nice to see the effects disentangled in the near future to be able to judge the sensitivity of QCD test in the scale breaking of the photon structure function.

3. Virtual Photon Structure Function

The first measurement of the structure function of a virtual photon target has been presented by PLUTO in the double tag mode. The target photon was tagged at small but finite angles resulting in a mean value of $\langle p^2 \rangle \equiv -\langle q_2^2 \rangle = 0.4$ GeV^2. The Q^2 range of the probe is similar to that in the single tag analysis, resulting in $\langle Q^2 \rangle = 6$ GeV^2. If both electrons are detected the kinematics of the process is completely known and the variables Q^2, p^2 and W can be determined from the scattered electrons. This procedure is almost independent on the fragmentation and the final state hadrons are only used for event definition (separation against the QED processes $\gamma\gamma \to ee, ee\gamma$). Only in the rare cases when W^2 comes out negative (due to finite energy resolution in the tagging systems) the final state hadrons are used to determine W.

The result is shown in Fig. 19 as a function of x and p^2. The data are in nice agreement with a superposition of the hadronic and pointlike component, where it makes almost no difference whether the pointlike component is calculated in the QM or in QCD. It is nice to see that the structure function drops with p^2 as expected (see eq. 9). For the p^2 dependence of the hadronic term a simple ρ-pole formfactor was assumed.

The comparison of the measurements and the models is only straightforward for the QM calculation as this calculation exists for the complete process $ee \to eeX$. The QCD calculations, however, are done for electron scattering off a (real or virtual) photon target[8], where the spin average is done over the incoming electron and photon. This leads to a formula with only two structure functions, F_2 and F_L, whereas the cross section for unpolarized electrons is given (after ϕ integration) by a four term formula (eq. 1). In the QM one can show that for $Q^2, p^2 \gg m_q^2$ the measurable cross section corresponds to[14]

$$\sigma = \frac{4\pi^2\alpha}{Q^2}\left(F_2 + \frac{3}{2}F_L\right). \qquad (14)$$

Therefore in Fig. 19 the longitudinal structure function (times 3/2) was added to F_2 in the QCD calculation. For the future it would be helpful

to have a QCD calculation for the whole process which could be directly compared to the measurements.

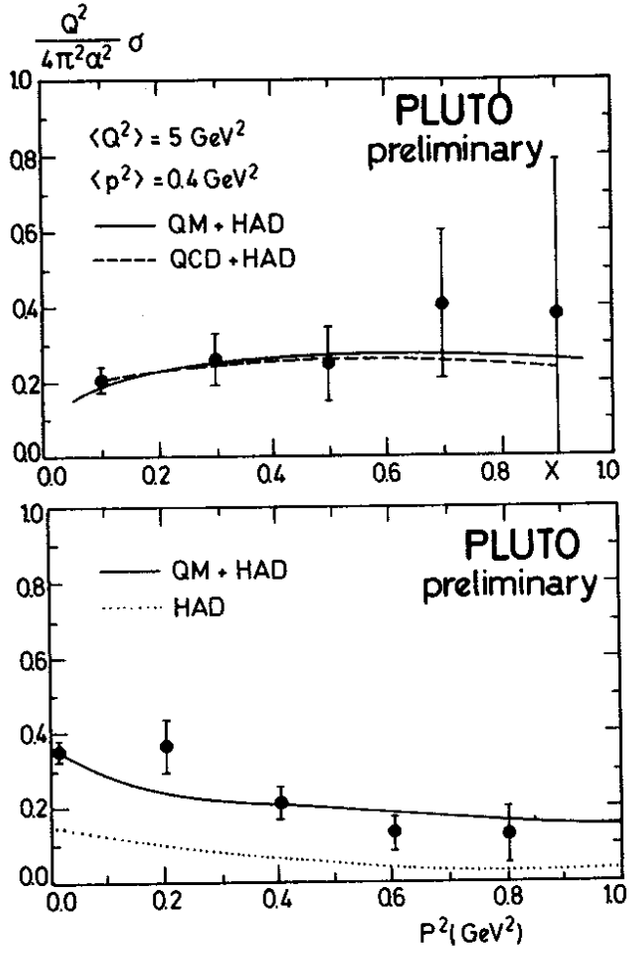

Fig. 19 Virtual photon structure function measured in the double tag mode (PLUTO) a) as a function of x averaged over Q^2 and p^2 and b) as a function of p^2 averaged over Q^2 and x

4. First Steps to Measure F_1 and F_3

The first attempt to disentangle the structure functions F_1 and F_2 has been tried by PLUTO, following the analysis of PEP 9 of the leptonic structure function[15]. From eq. 3 it is evident that the cross section is completely dominated by F_2 unless y is close to 1, corresponding to small energies of the scattered electron (eq. 5). PLUTO has lowered the minimum energy cut from 8 GeV (in the F_2 analysis) to 4 GeV, thus extending the y acceptance from 0.5 to 0.8 (see Fig. 20). The histogram represents the Monte Carlo expectation, where $F_1 = 0$ and the experimental structure function F_2, measured in the range $y < 0.4$, was used as an input. From the fact that the extrapolation of the pure F_2 term to large y-values does not account for the data one can conclude that F_1 does not vanish. But this statement is rather trivial as $F_1 = 0$ means that the

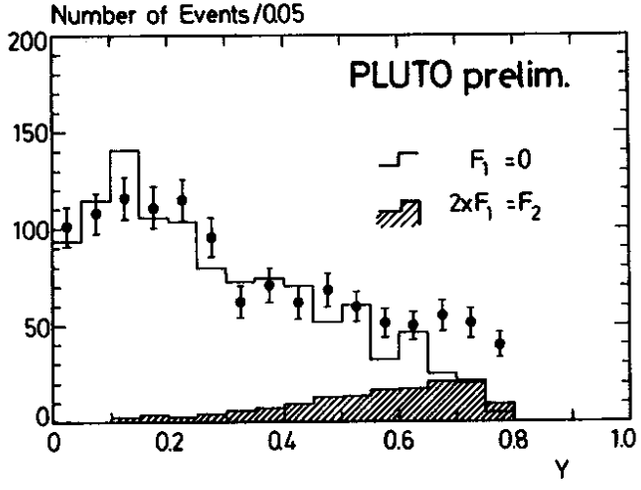

Fig. 20 y-distribution compared to Monte Carlo predictions for (1-y) F_2 and xy^2F_1 (PLUTO)

whole process is purely given by the longitudinal component (see eq. 4)

$$F_1 = F_T \qquad (15)$$

$$F_2 = 2 \times F_1 + F_\ell \,.$$

The other extreme is $F_\ell = 0$ in which case F_1 and F_2 are connected by the Callan-Gross relation[16]. In this case the shaded area has to be added to the histogram in Fig. 20, describing the data reasonably well. But I would hesitate to draw any firm conclusions about the F_ℓ term, as the analysis is still very preliminary and the background processes at low tag energies are still under study. A final analysis will include the electron identification with the gas Cerenkov Counter.

The first indication of a non vanishing F_3 term has been obtained in the analysis of double tag events by PLUTO. As F_3 is proportional to the interference term τ_{TT} in eq. 1 it can only be measured in double tag events, where it shows up as a ϕ modulation. Most of the data are

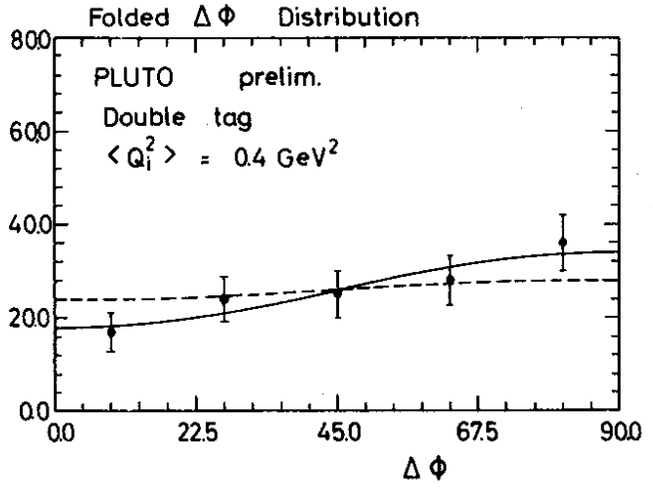

Fig. 21 $\Delta\phi$ distribution of the double tag events. The solid curve represents a fit of the typ A (1 + B cos 2ϕ)

coming from small angle tags (SAT - SAT coincidences), where the tagging system is completely ϕ symmetric. Thus the angle ϕ (= $\phi_{e^+} - \phi_{e^-}$), the angle between the e^+ and the e^- scattering planes in the $\gamma\gamma$ CMS, can be measured with uniform efficiency. Fig. 21 shows the distribution of the angle ϕ after folding to the interval 0 - 90°. The data are fitted by the form $A \cdot (1 + B \cos 2\phi)$. The result (solid curve)

$$B = -0.31 \pm 0.12 \qquad (16)$$

can be regarded as a first indication of the presence of a negative τ_{TT} term. The significance is marginal, about 2.5 standard derivations away from zero, and sign and magnitude agree with the QM prediction.

5. Conclusions

An enormous progress has been made during the last two years in the measurement of the photon structure function. The pointlike component of the photon has definitely shown up. Despite all the problems with QCD calculations the data are described by the very simple model 'hadronic part + leading order QCD, $\Lambda \approx 200$ MeV' in many respects: the shape in x as well as the absolute normalization of F_2^γ (x) agrees very well at moderate $\langle Q^2 \rangle$ values of 5.9. The Q^2 evolution has been studied up to several hundred GeV and is also consistent with this model. A detailed QCD test from the Q^2 evolution of F_2^γ, however, would require about ten times the statistic. I think, its worth the effort!

Acknowledgement

I am grateful to all my colleagues at PETRA and PEP for providing me with all the information and material needed for this review. I wish to thank the organizers, especially Jack Gunion and Dick Lander, for inviting me to such a beautiful and fruitful conference.

References

1 V.M. Budnev et al., Phys. Reports 15C (1975) 181

2 PLUTO collaboration Ch. Berger et al., Phys. Lett. 107B (1981) 168

3 I.F. Ginzburg and V.A. Serbo, Phys. Lett. 109B (1982) 231

4 A. Deuter, these proceedings

5 E. Witten, Nucl. Phys. B120 (1977) 189

6 D. Duke, these proceedings

7 W. Bardeen, discussion remark of the 5th Int. Workshop on Photon Photon Collision, Aachen (1983)

8 T. Uematzu and T.F. Walsh, Nucl. Phys. B199 (1982) 93

9 W. Wagner, PITHA 83/03

10 H. Spitzer, summary talk of the experimental session at the 5th Int. Workshop on Photon Photon Collisions, Aachen (1983), DESY report 83-059

11 F. Raupach, talk given at the 5th Int. Workshop on Photon Photon Collisions, Aachen (1983), summarized in ref. 10

12 CELLO collaboration, H.J. Behrend et al., DESY 83/018

13 W. Wagner, invited talk at the 5th Int. Workshop on Photon Photon Collisions, Aachen (1983), PITHA 83/17

14 This was pointed out by J. Dainton and S. Maxfield

15 M. Pohl, invited talk at the 5th Int. Workshop on Photon Photon Collisions, Aachen (1983), DESY report 83-047

16 C.G. Callan and D.J. Gross, Phys. Rev. Lett. 22(1969) 156

17 JADE Collaboration, W.Bartel et al., Phys.Lett. 121B (1983) 216.

RESONANCES IN TWO-PHOTON SCATTERING

Erwin Hilger

II. Institut für Experimentalphysik
Luruper Chaussee 149, D-2000 Hamburg 50, Germany

ABSTRACT

Measurements on resonance formation in collisions of two quasi-real photons are briefly summarized. The most recent experimental results are presented.

1. Introduction

The study of exclusive final states produced in photon-photon scattering has emerged as a very fruitful field of two-photon physics. In particular, on resonance formation many new results have become available recently.

This is a brief review of the status at the time of this conference. For more details we refer to the Proceedings of the $\gamma\gamma$-Workshop at Aachen, April 1983[1], especially to the articles by J.OLSSON, F.RENARD, and H.KOLANOSKI. Moreover, we concentrate on collisions of two quasi-real photons. Results on resonance production by one real and one virtual photon are reported by M.POPPE in these proceedings[2].

2. General Remarks

The process we deal with here is

$$e^+e^- \longrightarrow e^+e^-\gamma\gamma \longrightarrow e^+e^- \underset{\hookrightarrow \text{final state.}}{R}$$

Its cross section is proportional to the two-photon decay width of the resonance R and approx. proportional to the inverse of the 3rd power of its mass. At PEP/PETRA energies the production cross sections for the most prominent resonances η' or f are about 2 nb.

Resonances, in order to be produced by two photons, must be flavor neutral and must have positive C-parity. Since we consider photons that are predominantly real resonances with spin J = 1 are excluded by YANG's theorem[3].

The photons couple to the charges within the resonance, and the $\gamma\gamma$-width is therefore sensitive to the quark content. Due to this feature the $\gamma\gamma$ decay width of a resonance contains valuable information about its nature. Hence for meson spectroscopy the scattering of two quasi-real photons provides an important complement to hadronic production.

Ingrediences for the success of this branch of $\gamma\gamma$ physics are: the clean signature as a $\gamma\gamma$-reaction (low total energy, low multiplicities), the outstanding signature for the exclusive final state (transverse momentum balance), and in principle a sensitivity for all masses below $2 \cdot E_{beam}$ at the same time.

Detection efficiences, however, are mainly small as a consequence of the two-photon kinematics being unfavorable and detectors not being optimized for $\gamma\gamma$ reactions. They vary widely for different final states: ~15% for two-particle final states like $\pi^+\pi^-$ or $\gamma\gamma$, ~1% for $\pi^+\pi^-\gamma\gamma$ or $\pi^+\pi^-\pi^\circ$, and less than 1% for most others.

The yields are further reduced by the branching ratio of R to the observed final state. Low mass mesons usually have a dominant decay mode which can be chosen for detection. Heavy quark systems, however, tend to have many decay modes of comparable strength, which aggravates the problem of their detection (beyond the effect of their higher mass).

The outline of this article is determined by grouping the experimental results according to the type of resonance looked for:

- SU(3) states
- heavy quarkonium: η_c
- glueball candidates
- surprises.

3. $SU(3)_F$ Spectroscopy

The members of the standard SU(3) nonets that can be produced with real γ's have spin-parity 0^-, 0^+ and 2^+. As yet no scalar particle has been observed in $\gamma\gamma$ production.

3.1 Pseudoscalars

In the 0^{-+} nonet the neutral member with the lowest mass is the π^0. Already in 1960 F. LOW[4] proposed to measure its two-photon width in $\gamma\gamma$ scattering at an e^+e^- storage ring. That experiment is still to be done! For the π^0 a firm prediction exists from PCAC and the triangular anomaly:

$$\Gamma(\pi^0\to\gamma\gamma) = 7.6 \text{ eV}.$$

Experimentally the width is known from PRIMAKOFF production and lifetime measurements to be

$$\Gamma(\pi^0\to\gamma\gamma) = 7.95 \pm 0.55 \text{ eV}^{5)}.$$

At CERN a new experiment is under way to measure the π^0 lifetime to better than 1.5% by v.DARDEL, CRONIN and others[6]. Eventually this should reduce the error on $\Gamma_{\gamma\gamma}(\pi^0)$ to $\pm$ 0.1 eV. Two-photon scattering experimenters will have a hard time before they reach comparable accuracies.

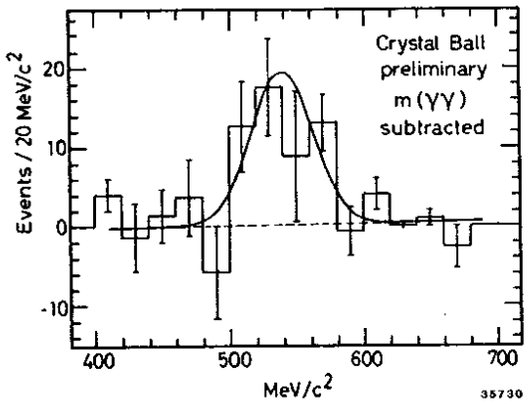

Figure 1. Subtracted $\gamma\gamma$ mass spectrum (CRYSTAL BALL)

The two-photon decay width of the η has been determined earlier in PRIMAKOFF experiments[5]. Recently the CRYSTAL BALL[1] at SPEAR has measured $\Gamma_{\gamma\gamma}(\eta)$ in the reaction

$$\gamma\gamma \longrightarrow \gamma\gamma.$$

For the first time elastic photon-photon scattering has now been observed. In an ambitious analysis the η signal was pulled out from a huge cosmic ray background. The two-photon mass distribution after subtraction of residual background determined from runs with separated beams is shown in Fig. 1.

There are 56 $\pm$ 12 events in the η range. The two-photon decay width comes out as

$$\Gamma_{\gamma\gamma}(\eta) = 0.56 \pm 0.12 \pm 0.09 \text{ keV} \quad \text{(CRYSTAL BALL prelim.)}$$

where the first error is statistical and the second is systematic. The value obtained is nearly two standard deviations larger than the latest PRIMAKOFF figure.

The η' resonance was the first one to be observed in $\gamma\gamma$ scattering, namely by MARK II at SPEAR[7] in 1979. Meanwhile there are measurements by many experiments[8)-10)]. They all studied the final state $\pi^+\pi^-\gamma$.

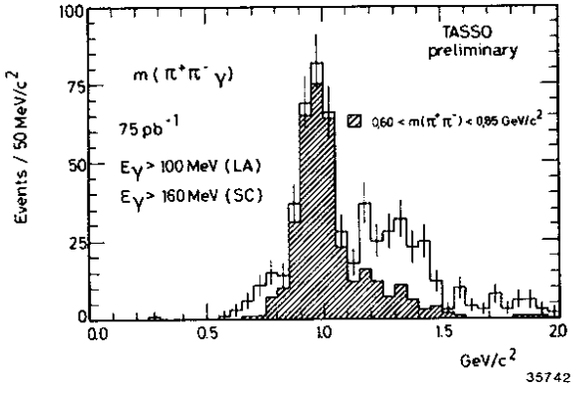

Figure 2. η' signal from TASSO (prelim.)

The most recent studies are from TASSO[1] (Fig. 2) and from PLUTO[2] (Fig.3). They are based on large event samples and employ the complete matrix element for the η' decay. Both experiments report preliminary values for $\Gamma_{\gamma\gamma}(\eta')$ that are somewhat smaller than previous results.

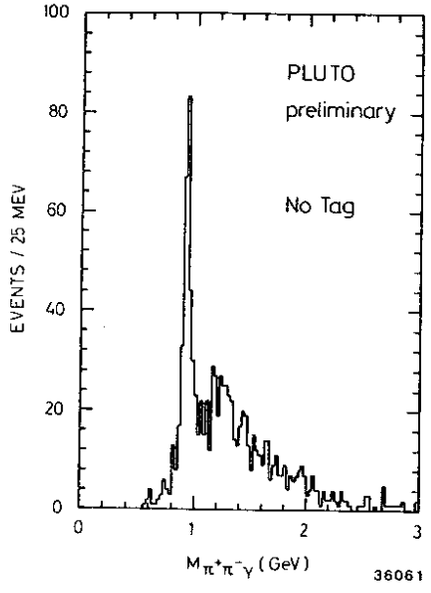

Figure 3. η' signal of PLUTO (prelim.)

The measured two-photon widths for the three 0^{-+} mesons are compiled in Table 1. The 0^{-+} mixing angle can be determined taking the weighted average of all available η' results. Different results are obtained depending on the value for the η decay width one uses in the evaluation: with the PRIMAKOFF width one gets $-10.2° \pm 3.1°$ which agrees with the $-11.2° \pm 0.2°$ obtained from the GELL-MANN - OKUBO quadratic mass formula[5]; using the new CRYSTAL BALL value leads to a more negative mixing angle of $-17.4° \pm 5°$ which is closer to the result $-18° \pm 2°$ as obtained from a recent mass matrix evaluation[11].

At present the uncertainties are still rather large and any conclusion would be premature. One should wait for the improved η' analyses and may be for another η measurement likely to be done by JADE. Note also that heavier isoscalar states, e.g. the $\iota(1440)$, may have to be included in the mixing scheme.

R	channel	$\Gamma(R\to\gamma\gamma)$ [keV]	Expt.	Ref.
π°		7.95±0.55 eV		5)
η	Primak.	0.324±.046	Cornell	5)
	$\gamma\gamma$	0.56±.12±.09	XTAL BALL	1)
η'	$\pi^+\pi^-\gamma$	5.8±1.1±1.2	MARK II	10)
		5.0±0.5±0.9	JADE	8)
		6.2±1.1±0.8	CELLO	9)
		4.1±0.4±1.5	TASSO prel.	1)
	average	5.3 ± 0.6 keV		

Table 1. Two-photon decay widths for pseudoscalar mesons

3.2 Tensor Mesons

The $SU(3)_F$ nonet of tensor mesons is long known to behave quite well with respect to SU(3) symmetry and the quark rules. All members are well established. The mixing of the two isoscalars f and f' is nearly ideal. The two-photon decay widths of the three flavor neutral members A_2, f, and f' have now all been measured in two-photon scattering.

The f(1270) was the first of these to be observed due to its dominant decay to the final state $\pi^+\pi^-$[12] which is convenient to measure. By now many experiments have determined $\Gamma_{\gamma\gamma}(f)$[1) 13)-16)]. The analysis of the f in the reaction $\gamma\gamma \to \pi^+\pi^-$ is impaired by the presence of a large continuum at low $\pi\pi$ invariant masses extending under the f signal. In $\gamma\gamma$ experiments the f appears with a shape dif-

ferent from that observed in hadronic reactions: the mass is shifted downwards by about 40 MeV.

Some of the early analyses were afflicted by improper treatment of the continuum (and some by trigger bias as well). A recent study of the $\pi^+\pi^-$ channel by CELLO[1] has helped to clarify the situation. The CELLO data correspond to 11.4 pb^{-1} integrated luminosity. A low bias two prong trigger was employed. QED contributions were calculated and subtracted after normalization to masses $M_{2\pi} > 1.8$ GeV, where hadron pairs are produced at a very small rate[17]. The contribution from K^+K^- to the data was estimated (from TASSO data) and subtracted. In Fig. 4 the f is seen sitting on a huge continuum and shifted in mass by about -60 MeV.

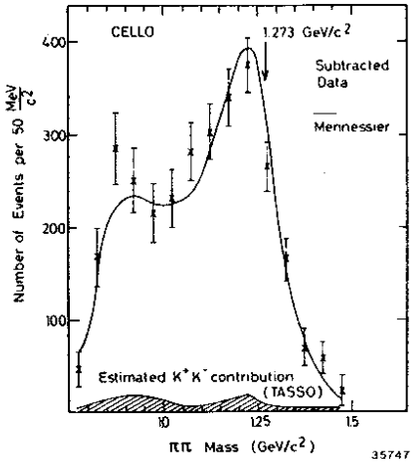

Figure 4. The f in $\gamma\gamma \to \pi^+\pi^-$ (CELLO).

The CELLO group used the MENNESSIER model[18] for their analysis. This approach to treat the reaction $\gamma\gamma \to \pi\pi$ is based on few theoretical assumptions only. It describes the production of pion and kaon pairs by real photons using a coupled channel formalism. Unitary corrections to account for the final state rescattering effects are taken from measured $\pi\pi$ and $K\bar{K}$ phase shifts and inelasticities. Then, only the strength of the vector meson (ω) exchange and the two-photon width of the f remain as free parameters.

The CELLO data are satisfactorily reproduced by neglegting the vector meson exchange. The mass plot is well described including the mass shift. The BORN amplitude is mainly helicity 2 and thus interferes strongly with the f. The mass shift comes out as observed if the interference is constructive below the f and destructive above. The one-parameter fit yields (assuming helicity 2 production of the f)

$$\Gamma_{\gamma\gamma}(f) = 2.7 \pm 0.2 \pm 0.2 \text{ keV} \quad \text{(CELLO prelim.)}.$$

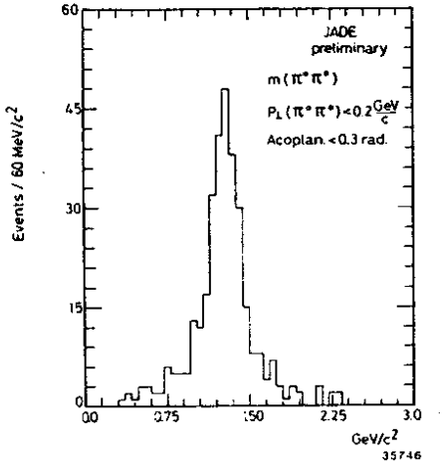

Figure 5. The f in $\gamma\gamma \to \pi^0\pi^0$ (JADE)

The f is also observed in the reaction $\gamma\gamma \to \pi^0\pi^0$ as known from the CRYSTAL BALL measurement[16]. Recently JADE[1] has studied this channel exploiting their neutral trigger on four photons in the final state with energies larger than 90 MeV each. Restricting the two-photon combinations to the π^0 region and plotting the invariant mass distribution of the two π^0s the f signal is seen with very little background (Fig. 5). A preliminary evaluation yields

$$\Gamma_{\gamma\gamma}(f) = 2.3 \pm 0.2 \pm 0.5 \text{ keV} \quad \text{(JADE prelim.)}.$$

Since in the $\pi^0\pi^0$ channel there is no direct BORN term the continuum is expected to be small. In the MENNESSIER model it results entirely from rescattering transforming $\pi^+\pi^-$ to $\pi^0\pi^0$. The parameters from the CELLO fit have been taken to calculate the neutral pion channel with this model. Again, the f comes out shifted downwards, by ~ 20 MeV, in agreement with the observation of the CRYSTAL BALL experiment.

The f'(1515) which predominantly contains strange quarks has recently been observed by TASSO[19] in $\gamma\gamma \to K\bar{K}$, with both charged and neutral kaons. Events with charged kaon pairs were identified as such via time of flight measurements. The K^+K^- mass plot in Fig. 6a shows a clear f' signal; in addition, at lower masses contributions are expected from the $K\bar{K}$ decays of f and A_2 as well as continuum production.

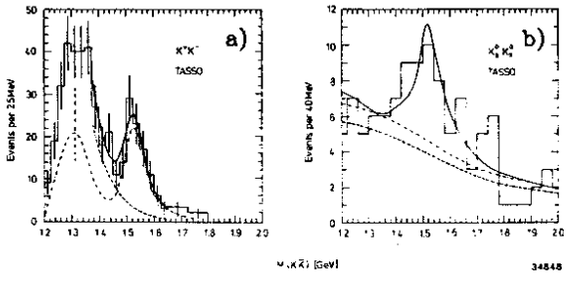

Figure 6. The f' in $\gamma\gamma \to$ a) K^+K^-, b) $K^0_sK^0_s$ (TASSO)

K^0_s's were detected via the $\pi^+\pi^-$ decay. Events of the final state $\pi^+\pi^-\pi^+\pi^-$ with two $\pi^+\pi^-$ combinations in the K^0 mass band were selected and kinematically fitted. The invariant mass distribution of the neutral kaon pairs in Fig. 6b shows the f' on top of background from other channels leading to a $\pi^+\pi^-\pi^+\pi^-$ final state. This background was determined from the side bands.

Contributions from f and A_2 are not negligible. In fact, for all three, f, A_2, and f', the product $\Gamma_{\gamma\gamma} \cdot BR_{KK}$ is of comparable size. Moreover, the three resonance contributions should add up coherently causing interference. The relative signs between the

amplitudes for f, f' and A_2 depend on the charge mode of the kaon pair they decay to. This is due to the different quark content of the tensor mesons and of the charged and neutral K's. For the K^+K^- case one expects constructive interference between f and A_2 while for K^0K^0 these amplitudes should interfere destructively. The data are consistent with this interference pattern. The two channels were analyzed independently and the results were found to be in good agreement. Combining both analyses TASSO obtained

$$\Gamma_{\gamma\gamma}(f') \cdot BR_{KK}(f') = 0.11 \pm 0.02 \pm 0.04 \text{ keV}$$

assuming helicity 2 production of tensor mesons. The branching ratio $BR(f' \to K\bar{K})$ has not yet been determined but is assumed to be large.

The $A_2(1320)$ has been observed in $\gamma\gamma$ scattering in different final states, first in $\gamma\gamma \to \eta\pi^0$ from $\gamma\gamma \to \gamma\gamma\gamma\gamma$ by the CRYSTAL BALL[18], then in $\gamma\gamma \to \rho\pi$ by CELLO[9].

A new analysis by JADE is now available based on the largest data sample obtained so far[1]. The observed final state is $\pi^+\pi^-\gamma\gamma$. The $\pi^\pm$'s are identified by dE/dx in the JADE chamber, the π^0's are reconstructed from two γ's and then constrained to the π^0 mass. After cuts a sample of 380 events for the reaction $\gamma\gamma \to \pi^+\pi^-\pi^0$ remains. The invariant mass distribution in Fig. 7 shows a nice A_2 signal, which is consistent with being produced entirely via the $\rho\pi$ decay mode.

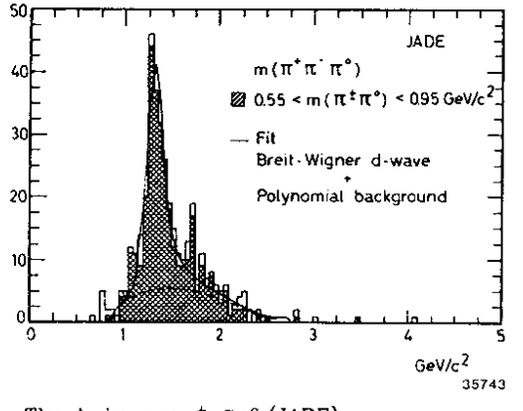

Figure 7. The A_2 in $\gamma\gamma \to \pi^+\pi^-\pi^0$ (JADE)

A fit to the A_2 with a polynomial background assigns 199 events to the A_2 and yields a width

$\Gamma_{\gamma\gamma}(A_2) = 0.84 \pm 0.07 \pm 0.15$ keV (JADE prelim.)

with the angular distributions indicating a dominant helicity $\lambda = 2$.

The results available on the two-photon decay widths of f, f', and A_2 are collected in Table 2. Weighted averages are also given.

R	channel	$\Gamma(R\to\gamma\gamma)$ [keV]	Expt.	Ref.
f	$\pi^+\pi^-$	2.3±0.5±0.35	PLUTO	13)
		3.2±0.2±0.5	TASSO	14)
		3.6±0.3±0.5	MARK II	15)
		2.7±0.2±0.2	CELLO prel.	1)
	$\pi^0\pi^0$	2.7±0.2±0.6	XTAL BALL	16)
		$2.9^{+0.2}_{-0.5}\pm0.6$	(hel.fit)	16)
		2.3±0.2±0.5	JADE prel.	1)
	average	2.8 ± 0.2 keV		
A_2	$\eta\pi^0$	0.77±0.18±0.27	XTAL BALL	16)
	$\rho\pi$	0.81±0.19±0.42	CELLO	9)
		0.84±0.07±0.15	JADE	1)
	average	0.82 ± 0.13 keV		
f'	KK	$\Gamma(f'\to\gamma\gamma)\cdot BR(f'\to K\bar{K})$		
		0.11±0.02±0.04	TASSO	19)

Table 2. Two-photon decay widths for tensor mesons

Helicity-2 dominance in the coupling of tensor mesons to two real photons is a prediction common to very different theoretical approaches and a standard input assumption to the analysis of most $\gamma\gamma$ experiments on tensor mesons. This assumption is necessary since the range of polar angles covered by the detectors is in most cases insufficient for a determination of the helicity structure. It is important because the acceptance depends strongly on the actual helicity mixture (factors up to 5 between $\lambda = 0$ and $\lambda = 2$). With realistic detectors an experimental determination of the helicity

structure is only possible with multiparticle final states. Helicity-2 dominance for $\gamma\gamma$ production of tensor mesons has been confirmed for $\gamma\gamma \to f \to \pi^0\pi^0$ by the CRYSTAL BALL[16]: $(\lambda = 2)/(\lambda = 0) \approx 9/1$ and now for $\gamma\gamma \to A_2 \to \rho\pi$ by JADE: $(\lambda = 2)/(\lambda = 0) \approx 9/1$ (preliminary).

For $\Gamma_{\gamma\gamma}(2^{++})$ there are no rigorous absolute predictions since the anomaly theorem can not be invoked. But ratios of decay widths are predictable from nonet symmetry, fractional charges and mixing angles. Such ratios are plotted in Fig. 8 as functions of the 2^{++} mixing angle. The case of $SU(3)_F$ being broken maximally, called 'ideal mixing', corresponds to an angle of 35.2°. Applying the GELL-MANN - OKUBO mass formula gives a mixing angle of 28°±3°. The ratios obtained from the present world average two-photon data are indicated as horizontal bands giving the one standard deviation uncertainty. The measured ratio $\Gamma_{\gamma\gamma}(A_2)/\Gamma_{\gamma\gamma}(f)$ appears to be on the low side compared to the SU(3) curve. However, this small difference may not persist as recent preliminary measurements of $\Gamma_{\gamma\gamma}(f)$ show a tendency to settle at values lower than obtained before. This would raise that ratio and eliminate the present difficulty.

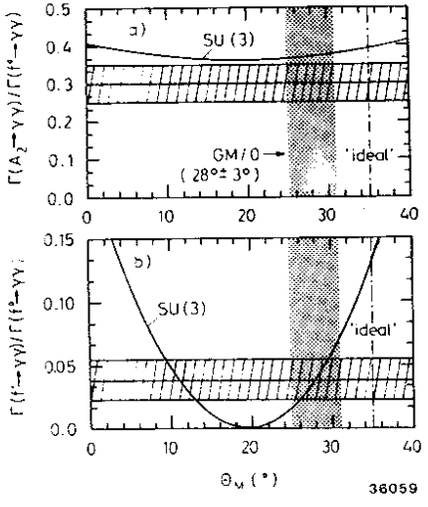

Figure 8. Ratios of $\gamma\gamma$ widths of tensor mesons

4. Heavy Quarkonium: η_c

Many theoretical predictions are available for $\Gamma_{\gamma\gamma}(\eta_c)$; they are listed in Table 3 and cluster around a notable 6 keV. Despite of all efforts of the experimenters the η_c has not yet been observed in $\gamma\gamma$ reactions.

$\Gamma(\eta \to \gamma\gamma)$ [keV]	Ref. 20)
~10	Barbieri et al
8.3 ± 0.7	Appelquist et al
1.6 ± 0.8	Shifman et al
6.4 ± 0.64	Aliev
5.6 ± 0.6	Kirschner et al
4.2 ± 0.4	Reinders et al

Table 3. : Predicted two-photon decay widths for the η_c meson.

From the searches for the η_c in various channels we present in Fig. 9 a recent mass distribution for the reaction $\gamma\gamma \to p\bar{p}$[21]. While the detection efficiency in the mass range of the η_c is reasonably high no event is observed. The available upper limits are listed in Table 4.

Channel	Upper limits	Expt.	Ref.
$BR(J/\psi\to\gamma\eta_c)\cdot BR_{\gamma\gamma}(\eta_c)$	$< 1.6\cdot10^{-5}$	XTAL BALL	22)
$\Gamma(\eta_c\to\gamma\gamma)\cdot BR_{2\pi\pm2\pi'}(\eta_c)$	< 4.2 keV	JADE	1)
$\Gamma(\eta_c\to\gamma\gamma)\cdot BR_{2\pi\pm\eta}(\eta_c)$	< 2.3 keV	JADE	1)
$\Gamma(\eta_c\to\gamma\gamma)\cdot BR_{p\bar{p}}(\eta_c)$	< 0.32 keV	TASSO	21)
$\Gamma(\eta_c\to\gamma\gamma)\cdot BR_{KK\pi}(\eta_c)$	< 27 keV	TASSO	1)
$\Gamma(\eta_c\to\gamma\gamma)\cdot BR_{2\pi+2\pi-}(\eta_c)$	< 0.7 keV	TASSO	1)

Table 4. : Upper limits on $\Gamma(\eta_c\to\gamma\gamma)$

The limit from the CRYSTAL BALL probably is the most restrictive one. The difficulty to observe the formation of the η_c in $\gamma\gamma$ reactions is related to the apparent absence of a dominant decay

mode of the η_c. Better knowledge of the η_c branching ratios is desired.

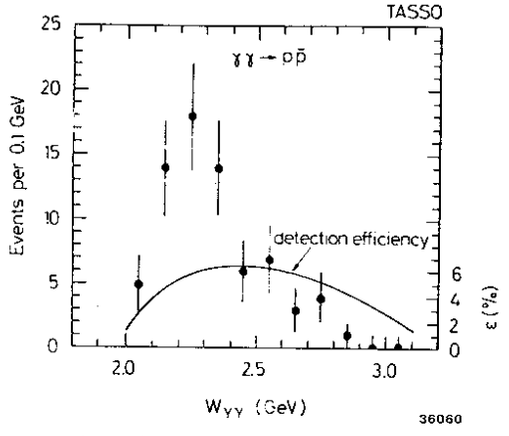

Figure 9. $p\bar{p}$ invariant mass distribution (TASSO)

5. Glueball candidates

The non-abelian nature of the widely accepted gauge model for the strong interactions, QCD, allows the existence of bound states of gluons, the glueballs. Such gluonium states may be found in the glueball favoring radiative decays of the J/ψ. Candidates are the $\iota(1440)$ seen to decay to $K\bar{K}\pi$ and the $\theta(1670)$ seen in the channels $\eta\eta$, $K\bar{K}$, $\eta\pi\pi$, and $\rho^0\rho^0$ with invariant mass peaks in the range 1640 to 1720 MeV. Possibly not all of these final states come from the same particle.

A pure glueball, G, contains no valence quarks, i.e. no charged constituents. Thus, its coupling to two photons is suppressed and $\Gamma_{\gamma\gamma}(G)$ should be much smaller than $\Gamma_{\gamma\gamma}(q\bar{q})$. It has to be expected, however, that the gluonium states mix with the isoscalar $q\bar{q}$ states of the same J^P quantum numbers. That will lead to physical states with detectable $\gamma\gamma$ widths. Hence, $\gamma\gamma$ reactions are complementary to radiative decays of heavy quarkonia for the determination of the glueball nature of new candidates and 'old' particles. Even upper limits for $\Gamma_{\gamma\gamma}$ could be of help to pin down the mixing pattern.

The $\iota(1440)$ is probably a 0^- state. There are many predictions for $\Gamma_{\gamma\gamma}(\iota)$ on the market[23] ranging from about 1 keV up to 12 keV. However, the ι has yet to be observed in $\gamma\gamma$ scattering. Some upper limits have been extracted from the data:

$\Gamma_{\gamma\gamma}(\iota) \cdot BR_{KK\pi}(\iota) < 8.0$ keV MARK II[24]
$\Gamma_{\gamma\gamma}(\iota) \cdot BR_{KK\pi}(\iota) < 7.0$ keV TASSO prelim.
$\Gamma_{\gamma\gamma}(\iota) \cdot BR_{\rho\rho}(\iota) < 1.0$ keV TASSO[25]
(all 95% c.l.)

If $K\bar{K}\pi$ is the dominant decay mode of the ι ($\geq$50%), then the limit from TASSO would correspond to $\Gamma_{\gamma\gamma}(\iota) < 15$ keV. If one trusts certain theoretical predictions the sensitivity required to actually see ι production in $\gamma\gamma$ scattering should soon be reached when over 150 pb^{-1} worth of data will have been collected.

For the 2^{++} glueball candidate $\theta(1650)$ the situation in $\gamma\gamma$ scattering is less favorable. The theoretical predictions around[25] agree roughly on $\Gamma_{\gamma\gamma}(\theta) < 1$ keV. This small value plus the fact that no dominant decay mode of the θ has been discovered may make it hard to observe the θ in $\gamma\gamma$ reactions. Hence, the presently available upper limits

$\Gamma_{\gamma\gamma}(\theta) \cdot BR_{KK}(\theta) < 0.4$ keV MARK II[24]
$\Gamma_{\gamma\gamma}(\theta) \cdot BR_{KK}(\theta) < 0.3$ keV TASSO[19]
$\Gamma_{\gamma\gamma}(\theta) \cdot BR_{\rho\rho}(\theta) < 1.2$ keV TASSO[25]
$\Gamma_{\gamma\gamma}(\theta) \cdot BR_{\eta\eta}(\theta) < 0.3$ keV CRYSTAL BALL[27]
(all 95% c.l.)

are far from being restrictive for the glueball nature of the θ. For models in which glueballs mix with $q\bar{q}$ states there is, however, already now important input from two-photon reactions since $\Gamma_{\gamma\gamma}(f')$ is very sensitive to the 2^{++} mixing pattern.

6. Surprises

This paragraph collects some recent findings in $\gamma\gamma$ reactions which came unexpected and for which an explanation is sought.

6.1 Threshold enhancement in $\gamma\gamma \to \rho^0\rho^0$

The strong enhancement in $\gamma\gamma \to 4\pi$ coming from the channel $\gamma\gamma \to \rho^0\rho^0$ reported by TASSO[28], MARK II[29], and CELLO[1] is still puzzling. Various speculations were offered mostly hypothesizing on reso-

nance production. In that case the final state would have well defined J^P and isospin.

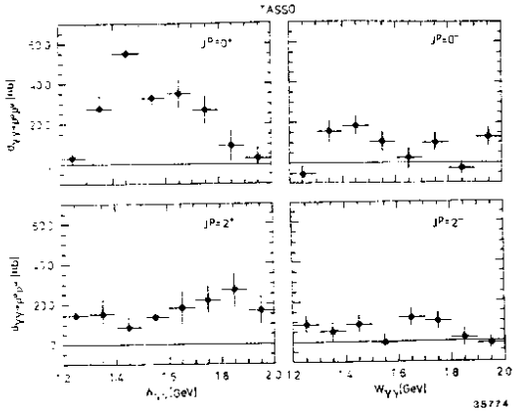

Figure 10. Decomposition of the cross section for $\gamma\gamma \to \rho^0\rho^0$ into different spin-parity contributions (TASSO)

The spin-parity analysis of TASSO[24] has been repeated as the original statistics has doubled meanwhile. It must be emphasized that the full matrix element is used including all mass and angular correlations. Maximum likelihood fits were made for $1.3 < M_{4\pi} \leq 2.0$ GeV. The new analysis confirms the findings of the published one in all aspects. Fig. 10 shows the decomposition of the cross section in the four lowest J^P states. Clearly, 0^- and 2^- do not play a dominant rôle. The 0^+ part is rather large for $M_{4\pi} < 1.8$ GeV, while 2^+ grows with $M_{4\pi}$ and dominates at $M_{4\pi} > 1.8$ GeV.

Important enlightment is expected from the production of other vector meson pairs. JADE[1] has determined a cross section for the process $\gamma\gamma \to \rho^+\rho^-$ from the final state $\pi^+\pi^-\pi^0\pi^0$. In Fig. 11 their result is compared to the TASSO cross section for $\rho^0\rho^0$ production (obtained assuming isotropic production and decay). Note that the $\rho^+\rho^-$ final state was not really identified and background was not subtracted. Therefore the JADE data rather represent upper limits to the $\rho^+\rho^-$ cross section. This, however, suffices to see that the

threshold behavior is very different for the two channels. No enhancement is present in the $\rho^+\rho^-$ channel,

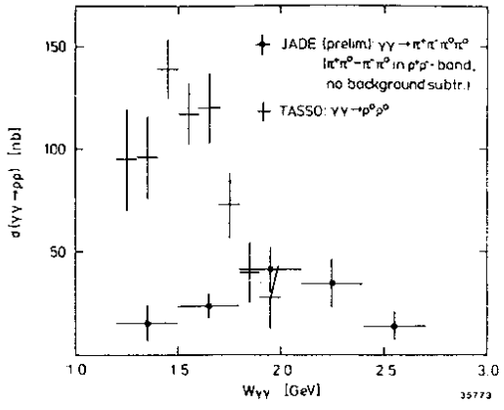

Figure 11. Comparison of $\rho^+\rho^-$ and $\rho^\circ\rho^\circ$ production in $\gamma\gamma$ scattering (JADE and TASSO)

The ratio $\sigma_{\gamma\gamma\to\rho^+\rho^-}/\ \sigma_{\gamma\gamma\to\rho^\circ\rho^\circ}$ can be evaluated for various mechanisms that could be responsible for the $\rho^\circ\rho^\circ$ enhancement:

isoscalar resonance	2
isotensor resonance	0.5
four-quark states	~ 0
VDM inspired models	~ 0.

With the new JADE result we can conclude that the $\rho^\circ\rho^\circ$ enhancement is certainly not due to an isoscalar resonance.

6.2 A signal at 2.1 GeV.

In the reaction $\gamma\gamma \to 4\pi$ TASSO has found a bump at $M_{4\pi}$ = 2.1 GeV[30]. The $M_{4\pi}$ mass plot in Fig.12 shows all the available data corresponding to 77 pb^{-1}.

A smooth curve was fitted to the mass spectrum between 1.65 and 3.0 GeV including the signal region. This fit leaves an excess between 2.05 and 2.15 GeV with a significance of 4.3σ. Adding a BREIT-WIGNER to the smooth background gives a good description of the data and yields 125.6 ± 46 events in the peak, centered at a mass

of 2103 ± 10 MeV and with a width of 30 ± 34 MeV. The 4π mass resolution of TASSO near 2 GeV of 60 MeV FWHM has been accounted for in the fit. Interpreting the signal as a resonance one gets

$$\Gamma_{\gamma\gamma}(\text{'2.1'})\cdot(2J+1)\cdot BR_{2\pi+2\pi-}(\text{'2.1'}) = 1.25\pm0.5\pm0.5 \text{ keV}.$$

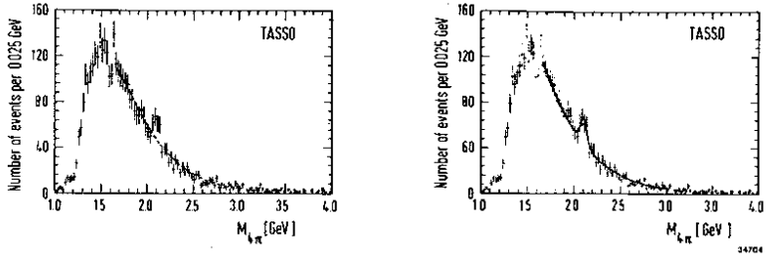

Figure 12. $M_{4\pi}$ distribution with the signal at 2.1 GeV (TASSO)

Further studies have shown that there is no correlation to the $\rho^\circ\rho^\circ$ portion of the 4π final state. Indeed, removing the events in the $\rho^\circ\rho^\circ$ band hardly affects the signal to background ratio (see Fig.13). There is no signal in the $K^\circ_s K^\circ_s$ fraction of the data.

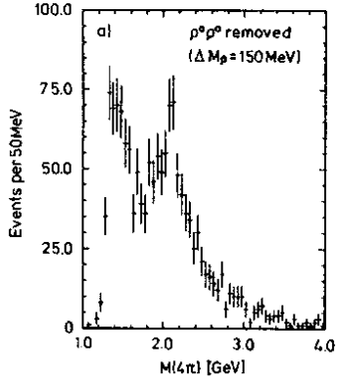

Figure 13. $M_{4\pi}$ distribution with ρ° bands subtracted (TASSO)

So far no other experiment investigating the reaction $\gamma\gamma\to\pi^+\pi^-\pi^+\pi^-$ has reported a signal in that mass region. However, most other detectors have a mass resolution inferior to TASSO.

MARK II, with a detector comparable to TASSO in mass resolution, nevertheless sees no indication of a bump around 2.1 GeV[31].

7. Summary

Resonance formation in collisions of quasi-real photons provides important tests of the quark charges and the quark content of flavor neutral mesons. The $\gamma\gamma$ decay widths of the corresponding members of the 0^{-+} and 2^{++} nonets are now all determined. So far no other known C = + mesons, neither the η_0 nor the scalars nor the glueball candidates ι and θ have been seen in $\gamma\gamma$ reactions. If one trusts theoretical prejudice, among those the ι will probably be observed first after a few more months of running at good luminosity. The large cross section found for $\gamma\gamma \to \rho^0\rho^0$ does not come from dominant resonance production. The signal seen in the $\pi^+\pi^-\pi^+\pi^-$ final state at 2.1 GeV by TASSO is not observed by other experiments.

Acknowledgements

In preparing my talk I have drawn heavily from the presentations given at the Aachen $\gamma\gamma$ Workshop and I have benefitted from frequent discussions with many colleagues, in particular, with H.Kolanoski, H.Kück, and J.Olssen. I am very much indepted to R.Lander for the assignment and to him and J. Gunion for a pleasent conference time.

References

1) Proceedings of the 5 th International Workshop on $\gamma\gamma$ Collisions, Aachen (April 1983)
2) M.Poppe, in these proceedings (Lake Tahoe 1983)
3) C.N.Yang, Phys.Rev.77(1950)242
4) F.Low, Phys.Rev.120(1960)582
5) Particle Data Group, Phys.Lett.111B(1982)
6) CERN-SPS proposal P177, experiment NA30
7) MARK II Coll., G.S.Abrams et al,Phys.Rev.Lett.43(1979)477
8) JADE Coll.,W.Bartel et al, Phys.Lett.113B(1982)190
9) CELLO Coll.,H.J.Behrend et al, Phys.Lett.114B(1982)378 (E)125B(1983)518
10) MARK II Coll., P.Jenni et al, Phys.Rev.D27(1983)1031
11) J.F.Donoghue, in Proceedings of the XVIII th Rencontre de Moriond (1983)
12) Ch.Berger, in Proceedings of the Intern. Conf. on $\gamma\gamma$ Collisions, Lake Tahoe (1979)
13) PLUTO Coll., Ch.Berger et al, Phys.Lett.94B(1980)254
14) TASSO Coll., R.Brandelik et al, Z.PhysikC10(1981)117
15) MARK II Coll., A.Roussarie et al, Phys.Lett.105B(1981)304
16) CRYSTAL BALL Coll., C.Edwards et al, Phys.Lett.110B(1982)82
17) PLUTO Coll., Ch.Berger et al, Nucl.Phys.B202(1982)189;and 1)
18) G.Mennessier, Z.Physik C16(1983)241
19) TASSO Coll., M.Althoff et al, Phys.Lett.121B(1983)216
20) R.Barbiero, R.Gatto, R.Kögerler, Phys.Lett. 60B(1976)183;
T.Appelquist, R.M.Barnett, K.Lane, Ann.Rev.Nucl.Sc.28(1978)387;
M.A.Shifman and M.Voisotsky, Z.Physik C10(1981)131;
T.M.Aliev, ITEP-76(1982);
R.Kirschner and A.Schiller, Z.Physik C16(1982)141;
L.J.Reinders, H.Rubinstein, S.Yazaki, Phys.Lett.113B(1982)411
21) TASSO Coll., M.Althoff et al, DESY 83-064(1983)
22) K.Königsmann, Proc. of the XVII th Rencontre de Moriond (1982)
23) K.Ishikawa, Phys.Rev.Lett.46(1981)978;
T.Teshima and S.Oneda, Phys.Lett.123B(1983)455;
C.Rosenzweig, A.Salomone, J.Schechter, Phys.Rev.D24(1981)2545;
S.Iwao, Lett.Nuov.Cim.35(1982)209;
K.A.Milton, W.F.Palmer and S.S.Pinsky, Phys.Rev.D27(1983)202
W.F.Palmer and S.S.Pinsky, Phys.Rev.D27(1983)2219
E.Kawai, Phys.Lett.124B(1983)262
24) D.L.Burke, in Proceedings of the XXI st Intern. Conf. on High Energy Physics, Paris (1982)
25) TASSO Coll., R.Brandelik et al, Z.Physik C16(1982)13
26) H.J.Schnitzer, Nucl.Phys.B207(1982)131;
J.L.Rosner, Phys.Rev.D24(1981)1347; Phys.Rev.D27(1983)1101
S.Iwao, Lett.Nuov.Cim.35(1982)481;
J.L.Rosner and S.F.Tuan, Phys.Rev.D27(1983)1544
27) K.Wacker, in Proc. of the XVIII th Rencontre de Moriond (1983)
28) TASSO Coll., R.Brandelik et al, Phys.Lett. 97B(1980)448
29) MARK II Coll., D.L.Burke et al, Phys.Lett.103B(1981)153
30) D.Lüke, in Proceedings of the XXI st Intern. Conf. on High Energy Physics, Paris (1982)
31) Mark II Coll., private communication

Q^2 DEPENDENCE OF SINGLE MESON PRODUCTION IN $\gamma\gamma$ COLLISIONS

Martin Poppe
Universität Hamburg
DESY - F14
Notkestrasse 85
D 2000 Hamburg 52

Abstract

New results from the PLUTO collaboration on η' production as a function of Q^2 in two photon fusion will be presented. A brief discussion of models is also included.

Introduction

The production of a single meson in the reaction $e^+e^- \to e^+e^-$ m can be interpreted as a two step process:

$$e^+e^- \to e^+e^- \gamma\gamma,$$
$$\gamma\gamma \to m \to \text{decay products}$$

(see fig.1). Throughout this text, the $\gamma\gamma$ cross section will be defined such that the corresponding e^+e^- cross section can be obtained by using the flux factors given by Budnev et al [1]).

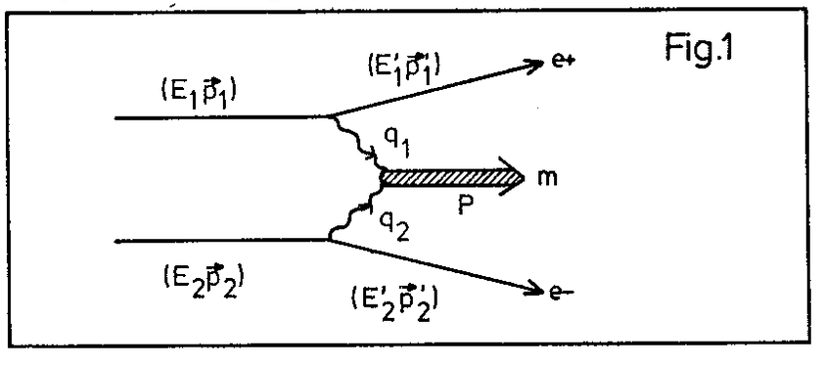

In general, both photons are virtual. However, if the scattering angles of the electrons are small, the masses of the two photons are negligible compared with all other energy scales involved. In this case, the second step of the reaction is considered to be the collision of quasi real photons (see fig.1). If Q^2 is much smaller than the mass squared of the meson, the cross section is just proportional to the two photon width, $\Gamma_{\gamma\gamma}$, of the resonance:

$$\sigma_{\gamma\gamma} = \frac{8\pi}{m} E_{\gamma\gamma} \frac{\Gamma_{\gamma\gamma}\Gamma}{(s-m^2)^2+\Gamma^2m^2} (2J+1)$$

where $E_{\gamma\gamma}=\sqrt{s}$ is the c.m.s. energy of the $\gamma\gamma$ system. This relation is frequently used to turn e^+e^- cross sections into measurements of the two photon width of a resonance.

Finally, it should be pointed out that, as soon as Q^2 is no longer negligible, the width is no longer a good variable, since the interchange of flux factors and phase space elements leads to rather awkward distortions. Better variables are either the $\gamma\gamma$ cross section, or the photon transition form factor F, which measures the deviation from the production of a pointlike meson. A full treatment of the form factor formalism can be found in reference [2]). For the 0^- nonet, the form factor is related to the two photon cross section via

$$\sigma_{\gamma\gamma}^* = \frac{1}{4\sqrt{X}} (\nu^2-m^2\tilde{Q}^2)F^2 \frac{E_{\gamma\gamma}\Gamma}{(s-m^2)^2+\Gamma^2m^2}$$

where $\sqrt{X}$ is Moeller's flux factor:

$$X \equiv (q_1\cdot q_2)^2 - q_1^2q_2^2,$$

$\tilde{Q}$ is defined as $(q_1-q_2)/2$ and $\nu\equiv\tilde{Q}\cdot P$. Note that the form factor has the dimension of a length.

Experimentally, the decay products of the meson are observed. In the PLUTO detector, electrons scattered by more than 30 mrad are seen as well. In this case, the event is said to be "tagged". Since $Q^2\equiv -q^2 \approx E\cdot E'\cdot\vartheta^2$, a tagged event comes from the interaction of a quasi real and a virtual photon, the latter having $Q^2 \geq 0.1$ GeV^2 at

PEP/PETRA energies. Photons with a Q^2 larger than this value are labelled conventionally with an asterik, i.e. γ^*.

Models

If we interpret the $\gamma\gamma$ vertex in the context of the quark parton model (see fig. 2), we end up with a diagram involving one incalculable vertex (v_m) only [2].

Fig.2

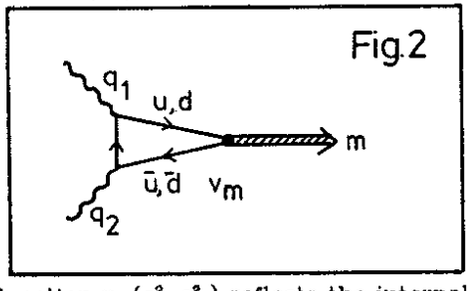

The vertex function $v_m(q^2_1,q^2_2)$ reflects the internal structure of the meson. Thus, the Q^2 evolution of the $\gamma\gamma^* \rightarrow$ meson cross section is an indirect measure of the quark structure of mesons.

Recently, Brodsky and Lepage have made a prediction for the $\gamma\gamma^*$ cross section in the framework of perturbative QCD. According to their analysis, the cross section for the case $Q^2 \rightarrow \infty$ can be expressed in terms of the meson decay constant f_m(i.e. a quantity which is measured at $Q^2 = 0$), leaving the meson wave function as the only unknown. For the 0^- nonet, their asymptotic prediction is

$$F_m \rightarrow 8\pi\alpha f_m/Q^2 \quad (\text{for } Q^2\rightarrow\infty).$$

If one assumes that the decay $m \rightarrow \gamma\gamma$ is due to a predominantly pointlike process, the decay constant can be determined from the two photon width of the meson. In case of the π^0, this seems to work [3], for other mesons, the situation is less clear (see Hilger's talk in these proceedings).

This leads us to the mechanism which might well dominate the experimentally accessible (low Q^2) world. It is known from photoproduction and electroproduction measurements that photons

frequently turn into vector mesons before they interact with hadronic matter. These transitions lead to characteristic form factors (see fig.3).

Fig. 3

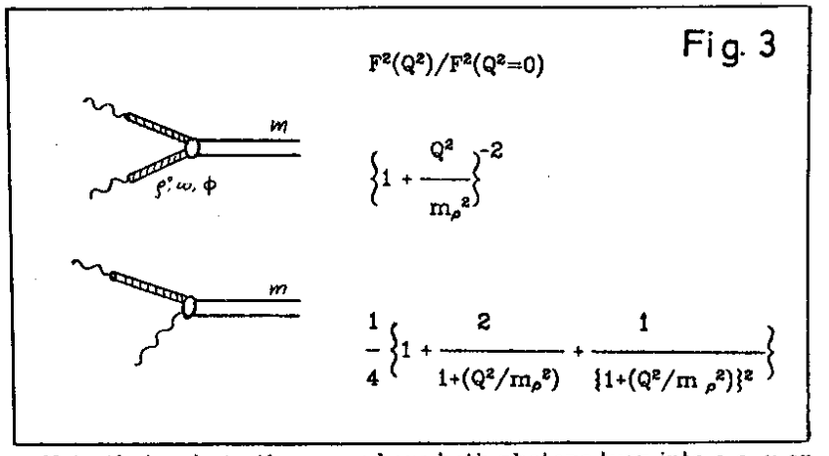

Note that only in the case where both photons turn into a ρ, ω or φ, the full vector meson propagator is expected. This diagram has another interesting feature: since its central bit is entirely hadronic, all isospin selection rules apply. Thus, for the reaction $\gamma\gamma \rightarrow A_2$, the $\rho\rho$, $\omega\omega$ and $\varphi\varphi$ diagrams are forbidden. Since only a small number of resonances is affected by these restrictions, a comparison between different mesons might provide the clue as to whether or not vector meson terms really lead to cross sections different from pointlike ones.

If only one of the initial photons transforms into a vector meson, the amplitude is the sum of two symmetric terms, leading to a $\gamma^*\gamma$ cross section involving a rho pole, an interference term and a constant. The constant term corresponds to the case where only the on-shell photon turns into a vector meson. By comparison of the different form factor terms, we see that in different $\{Q^2_1,Q^2_2\}$ domains, different mechanisms may contribute.

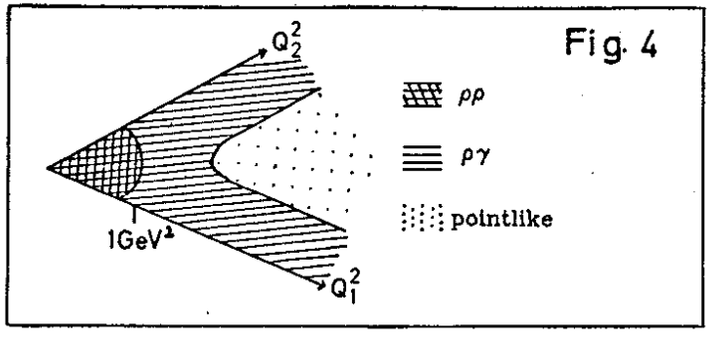

First measurement of the η' form factor

This analysis is based on 25pb^{-1}, taken by the PLUTO detector at a PETRA beam energy of 17.5 GeV. The data selection aimed for

a) full trigger efficiency:
$|\cos(\pi,\text{beam})| < 0.8$
at least 1 track with $p_\perp > 150$ MeV

b) background minimisation:
$\cos(\pi,\gamma) < 0.9$ → no radiating electrons
$\cos(\pi^+,\pi^-) < 0.9$ → no Dalitz pairs
$p_\perp^2(\text{tag}+\pi^+ +\pi^-) > 0.02$ GeV^2 → no fake photons
χ^2(2 C fit) → no incomplete multiprongs.

Here, cos(a,b) is the cosine of the angle between particles "a" and "b" at the interaction point in the lab frame. The mass spectrum of the 209 events remaining after these cuts is shown in fig.5.
There is an enhancement at the mass of the η'. The hypothesis of this being a genuine signal is supported by the fact that it is correlated with a ρ^0 signal in the $\pi^+\pi^-$ mass spectrum (see fig.5 and fig.6).

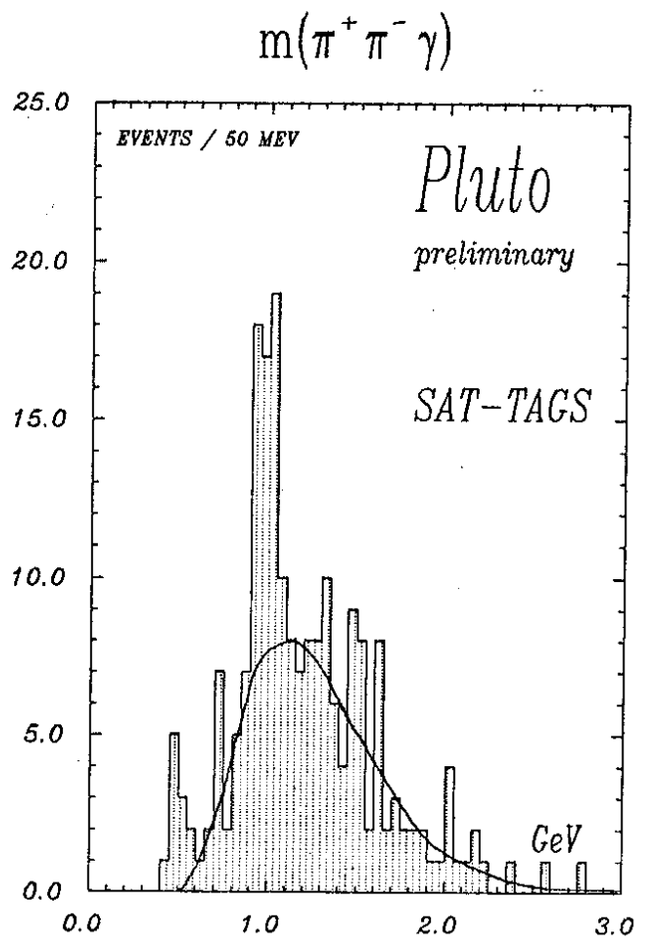

Figure 5: Invariant mass spectrum of $\pi^+\pi^-\gamma$ events. The mean Q^2 is 0.4 GeV^2

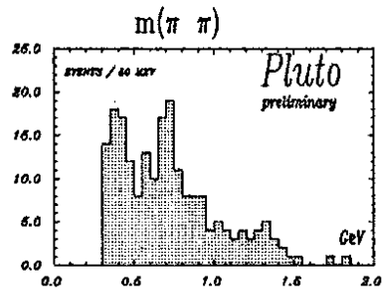

Figure 6: Mass distribution of $\pi\pi$ system in the above sample

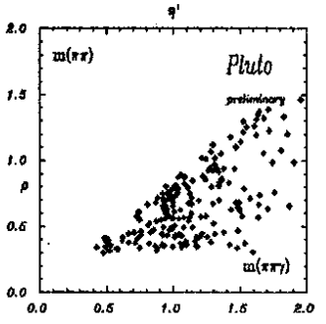

Figure 7: Correlation between the $\pi\pi\gamma$ mass and the $\pi\pi$ spectrum

Acceptance calculation

For the determination of the cross section, a Vermaseren Monte Carlo program was used to generate the photon flux. The fusion cross section was assumed to be of the form given in the introduction with a constant form factor. The decay $\eta' \to \rho\gamma$ was modelled such that $|M|^2 \sim E_\gamma^2$ where E_γ is the energy of the photon in the η' rest frame [6]). The ρ mass spectrum was generated according to a prescription given by J. D. Jackson [4]):

$$\frac{d\Gamma(\eta'\to\rho^0\gamma)}{dm_\rho^2} \approx E_\gamma |M|^2 \frac{m_0\Gamma(m_\rho)}{(m_0^2-m_\rho^2)^2 + m_0^2\Gamma_\rho^2(m_\rho)}$$

The additional E_γ factor comes from the η' phase space, m_0 is the nominal ρ^0 mass (770 MeV), and

$$\Gamma(m_\rho) = \Gamma(m_0)\left\{\frac{E_\gamma(m_\rho)}{E_\gamma(m_0)}\right\}^3 \frac{p^*(m_\rho)}{p^*(m_0)}$$

with

$$p^*(m_\rho) \sim \{q_0^2+q_\rho^2\}^{-1},$$

q being the π momentum in the ρ^0 rest frame. The helicities of the ρ^0's were assumed to be an equal mixture of ±1 in the η' rest frame. A comparison with the data gives the transition form factor shown in fig. 7. The point at $Q^2=0$ corresponds to a width of 3.8 keV.

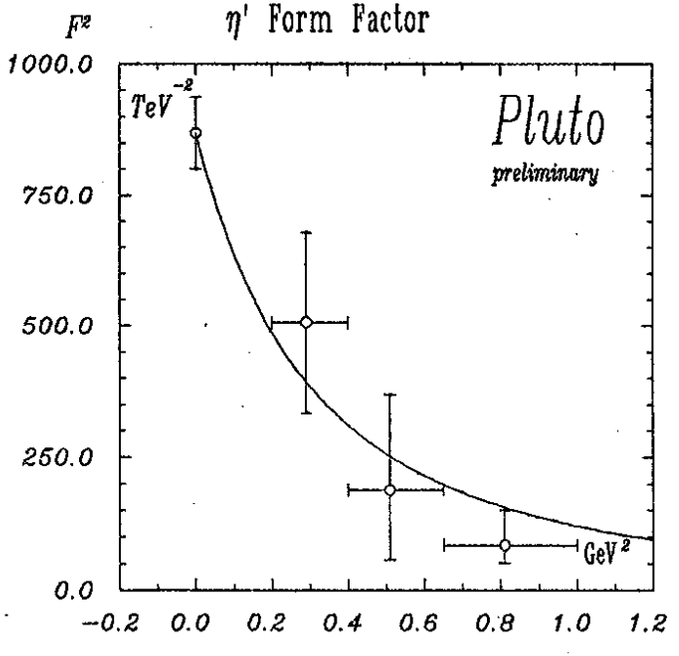

Figure 8: The $\gamma\gamma \to \eta'$ transition form factor squared as a function of Q^2. The errors shown are statistical only. The curve is a simple ρ pole.

Unfortunately, the data do not extend to high enough Q^2, so that a destinction between vector dominance, ρ^0 excitation and QCD cannot be made. The situation might improve considerably, if the systematic errors of $\Gamma_{\gamma\gamma}$ measurements are reduced, and if recently found double tagged events are turned into a cross section as well (see fig.9).

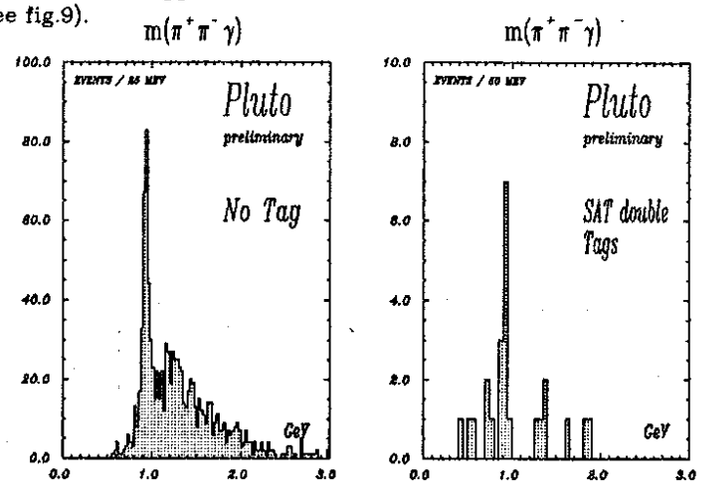

Figure 9: η' signals in no tag and double tag events.

Aknowledgment

I would like to thank all PLUTO members for help and discussion.

References

1) V.M. Budnev et al
Phys. Reports 15 No4 (1975) 181

2) G. Koepp, T. Walsh and P.Zerwas
Nuclear Physics B70 (1974) 461

3) S.L. Adler
Phys. Review 177 No5 (1969) 2426

4) S.J. Brodsky and J.P. Lepage
Phys. Review D 24 No7 (1981) 1801
(when using B.&L.'s paper in connection with standard photon fluxes and cross sections, multiply their form factor by $4\pi\alpha$)

5) J.D. Jackson
Il Nuovo Cimento 34 No6 (1964) 1644

6) The E_γ^2 factor comes from the spins involved. The resulting shift in the ρ^0 mass is also been seen experimentally. (Allan Rittenberg: PhD thesis on "Properties of the η'", LBL)